

---

# Implicit Degree Bias in the Link Prediction Task

---

Rachith Aiyappa<sup>1</sup> Xin Wang<sup>2</sup> Munjung Kim<sup>1</sup> Ozgur Can Seckin<sup>1</sup> Yong-Yeol Ahn<sup>1</sup> Sadamori Kojaku<sup>2</sup>

## Abstract

Link prediction—the task of distinguishing actual hidden edges from random unconnected node pairs—is a quintessential task in graph machine learning. Despite being widely accepted as a universal benchmark and a downstream task for representation learning, its validity is seldom questioned. Here, we show that the common edge sampling procedure in link prediction introduces an implicit bias toward high-degree nodes and produces a skewed evaluation that favors methods overly reliant on node degree, to the extent that a “null” method based solely on node degree can nearly match optimal performance. To address this, we propose a degree-corrected link prediction task that offers a more accurate assessment that aligns better with performance in recommendation tasks. Finally, we demonstrate that this degree-corrected benchmark can more effectively train graph machine-learning models by reducing overfitting to node degrees and facilitating the learning of relevant structures in graphs.

## 1. Introduction

Standardized benchmarks like ImageNet (Deng et al., 2009; Krizhevsky et al., 2012) and SQuAD (Rajpurkar et al., 2016; 2018) play a pivotal role in driving progress in machine learning by fostering competition through setting clear, measurable goals. In graph machine learning, a core benchmark is link prediction, which involves identifying missing edges in a graph, with diverse applications including the recommendations of friends and contents (Huang et al., 2005; Kunegis & Lommatzsch, 2009; Menon & Elkan, 2011; Wang et al., 2014), knowledge discoveries (Bordes et al.,

2013; Sun et al., 2019), and drug development (Wang et al., 2015; Crichton et al., 2018; You et al., 2019; Ali et al., 2019; Breit et al., 2020; Yue et al., 2020; Abbas et al., 2021). Link prediction benchmarks have been essential for quantitative evaluations, advancing graph machine learning techniques (Liben-Nowell & Kleinberg, 2003; Narayanan et al., 2011; Ali et al., 2019; Ghasemian et al., 2020; Mara et al., 2020; Breit et al., 2020; Yue et al., 2020).

Despite its significant role in graph machine learning, the link prediction benchmark itself is rarely scrutinized for effectiveness, reliability, and bias. Typically, it evaluates methods based on their ability to classify node pairs as connected or unconnected (Kunegis & Lommatzsch, 2009; Ghasemian et al., 2020; Mara et al., 2020). Connected pairs (edges) are randomly sampled from existing edges as the hidden positive set, while an equal number of unconnected node pairs are sampled randomly. Criticisms often highlight its disconnect from real-world scenarios. For instance, unconnected pairs vastly outnumber connected ones because of the graph sparsity (Barabási & Pósfai, 2016; Newman, 2018), leading to biased performance evaluations (Yang et al., 2015; Wang et al., 2021; Huang et al., 2023; Li et al., 2024a; Menand & Seshadhri, 2024). Additionally, the benchmark tests a predefined set of edges, while real-world tasks involve identifying potential edges across the entire graph. Despite this misalignment, high benchmark performance is often seen as a marker of successful learning in graph machine learning (Ou et al., 2016; Grover & Leskovec, 2016; Goyal & Ferrara, 2018; Crichton et al., 2018; Zhang & Chen, 2018; Ali et al., 2019; Breit et al., 2020; Ghasemian et al., 2020; Yue et al., 2020; Cai et al., 2021).

Here, we argue that the standard link prediction benchmark has a fundamental and severe bias favoring methods that exploit node degree (the number of edges a node has). This bias arises from the edge sampling process: a node with  $k$  edges is  $k$  times more likely to be selected than a node with a single edge ( $k = 1$ ). Meanwhile, the negative set is randomly sampled from unconnected pairs, without this degree bias. This creates a distinct feature (degree) that methods can exploit without understanding any non-trivial structural features of the graph. We show that this degree bias is so profound that a “null” method based solely on node degree can achieve near-optimal performance, questioning the benchmark’s usefulness as a general objective in

\*Equal contribution <sup>1</sup>Center for Complex Networks and Systems Research, Luddy School of Informatics, Computing, and Engineering, Indiana University, Bloomington, IN, USA <sup>2</sup>School of Systems Science and Industrial Engineering, Binghamton University, Binghamton, NY, USA. Correspondence to: Sadamori Kojaku <[skojaku@binghamton.edu](mailto:skojaku@binghamton.edu)>.

graph machine learning and highlighting the need for being more intentional and careful about what the evaluation tasks themselves actually evaluate.

To address this bias, we propose a degree-corrected link prediction benchmark that samples unconnected node pairs with the same degree bias. This benchmark more accurately reflects the performance of algorithms in recommendation tasks. Moreover, it trains graph neural networks more effectively by reducing overfitting to node degrees, thereby improving the learning of community structure in graphs.

## 2. Design flaw of the link prediction benchmark

### 2.1. Preliminary

We focus on unweighted, undirected graph  $G = (\mathcal{V}, \mathcal{E})$ , where  $\mathcal{V}$  is the set of nodes and  $\mathcal{E}$  is the set of edges. We assume that  $G$  has no self-loops, no multiple edges, and is highly sparse ( $|\mathcal{E}| \ll |\mathcal{V}|^2$ ), a common characteristic of real-world graphs (Barabási & Pósfai, 2016; Newman, 2018). Degree  $k_i$  of a node  $i \in \mathcal{V}$  is the number of edges connected to it. We use  $\sim$  to denote proportional relationships. Node attributes, if present, are excluded to maintain consistency across all link prediction methods.

### 2.2. Link prediction benchmark

The standard link prediction benchmark procedure is as follows (Kunegis & Lommatzsch, 2009; Grover & Leskovec, 2016; Ou et al., 2016; Zhang & Chen, 2018; Crichton et al., 2018; Goyal & Ferrara, 2018; Ali et al., 2019; Breit et al., 2020; Yue et al., 2020; Cai et al., 2021). First, a fraction  $\beta$  of edges is randomly sampled from the edge set  $\mathcal{E}$  as *positive edges*. Second, an equal number of unconnected node pairs is randomly sampled with replacement from the node-set  $\mathcal{V}$  as *negative edges*. Negative edges are resampled if they form a loop or are already in the positive or test edges. Third, each node pair  $(i, j)$  is scored by a link prediction method, where a higher score  $s_{ij}$  indicates a greater likelihood of an edge. Fourth, the method’s effectiveness is evaluated using the Area Under the Receiver Operating Characteristic Curve (AUC-ROC), which represents the probability that the method gives a higher score to a positive edge than a negative edge. While alternative benchmark designs use different evaluation metrics or sampling strategies for negative edges (Yang et al., 2015; Wang et al., 2021; Wang & Derr, 2022; Huang et al., 2023; Russo et al., 2024; He et al., 2024; Li et al., 2024a; Menand & Seshadhri, 2024) (Section 4), this outlined procedure is widely adopted (Kunegis & Lommatzsch, 2009; Grover & Leskovec, 2016; Ou et al., 2016; Goyal & Ferrara, 2018; Zhang & Chen, 2018; Crichton et al., 2018; Ali et al., 2019; Breit et al., 2020; Yue et al., 2020; Ghasemian et al., 2020).

### 2.3. Sampling bias due to node degree

A well-known, counterintuitive fact about graphs is that a uniform random sampling of edges introduces a *degree bias* in node selection (Feld, 1991; Barthélémy et al., 2004; Christakis & Fowler, 2010; Kojaku et al., 2021a;b). The bias arises because a node with  $k$  edges appears  $k$  times in the edge list and thus  $k$  times more likely to be chosen than a node with  $k' = 1$  edge (e.g., node 1 and 4 in Fig. 1A). Consequently, for a graph with degree distribution  $p(k)$ , the nodes in the positive edges have degree distribution  $p_{\text{pos}}(k)$  proportional to  $\sim k \cdot p(k)$ . By normalizing  $k \cdot p(k)$ , the degree distribution of the positive edges is given by

$$p_{\text{pos}}(k) = \frac{1}{\sum_{\ell} \ell p(\ell)} k \cdot p(k) = \frac{1}{\langle k \rangle} k \cdot p(k), \quad (1)$$

where  $\langle k \rangle$  is the average degree. By contrast, nodes in the negative edges are uniformly sampled from the node-set  $\mathcal{V}$ , resulting in a degree distribution  $p_{\text{neg}}(k)$  identical to  $p(k)$  (i.e.,  $p_{\text{neg}}(k) = p(k)$ ).

We demonstrate the degree bias using the Price graph with  $N = 10^5$  nodes and  $M = 10^6$  edges, which follows a power-law degree distribution  $p(k) \propto k^{-3}$  (Fig. 1B). We uniformly sample  $\beta = 0.25$  of the edges from  $\mathcal{E}$  as positive edges, together with an equal number of unconnected node pairs sampled uniformly from  $\mathcal{V}$ . The degree distributions for nodes in the positive and negative edges align with  $p_{\text{pos}}(k)$  and  $p_{\text{neg}}(k)$ , respectively, confirming the sampling bias due to node degree. This degree bias is not specific to the Price graph but occurs in any graph with a non-uniform degree distribution.

### 2.4. Impact of degree bias on the link prediction benchmark

We demonstrate the impact of degree bias on link prediction benchmarks (Fig. 1D) by evaluating 29 link prediction methods across 95 graphs from various domains, including social, technological, informational, biological, and transportation graphs. These methods include 7 network topology-based methods (e.g., Common Neighbors (CN) (Liben-Nowell & Kleinberg, 2003)), 13 graph embedding methods (e.g., Laplacian EigenMap (EigenMap) (Belkin & Niyogi, 2003)), 2 network models (e.g., Stochastic Block Model (e.g., SBM) (Fortunato, 2010)), and 4 graph neural networks (GNNs) (e.g., Graph Convolutional Network (GCN) (Kipf & Welling, 2017)). Detailed method and graph descriptions are available in Appendix A. We set the test edge fraction to  $\beta = 0.25$  and repeat the experiment 5 times. We quantify the heterogeneity  $\sigma$  of node degree by fitting a log-normal distribution to  $p(k)$  and calculating its variance parameter  $\sigma$ . We will show that  $\sigma$  is a reliable indicator of the impact of degree bias in Section 2.5.

We focus on the Preferential Attachment (PA) link predic-

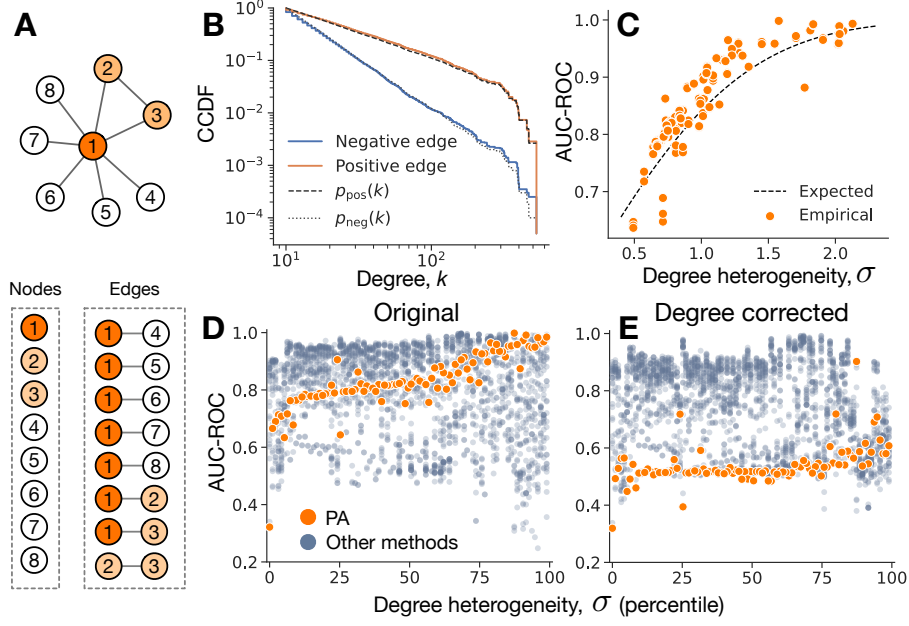


**Figure 1.** Illustration of the degree bias in the link prediction benchmark. **A:** A node with degree  $k$  appears  $k$  times in the edge list, making it  $k$  times more likely to be sampled as a positive edge than a node with degree 1. **B:** The degree distribution of the nodes in the positive and negative edges sampled from a Price graph of  $N = 10^5$  nodes and  $M = 10^6$  edges. The y-axis, ‘‘CCDF’’, denotes the complementary cumulative distribution function, representing the probability that a node’s degree is at least  $k$ . Dashed lines illustrate the relationship described by Eq. 1. **C:** The AUC-ROC score for the Preferential Attachment (PA) method on empirical graphs, with the dashed line indicating Eq. 4. **D:** AUC-ROC of 29 methods across 95 graphs. **E:** AUC-ROC of the same methods for the degree-corrected benchmark.

tion method, which calculates the prediction score  $s_{ij} = k_i k_j$  using only node degrees. PA is a crude method that neglects key predictive features like common neighbors and shortest distance (Li et al., 2024a; Menand & Seshadri, 2024; Lichtnwalter & Chawla, 2012; Zhang & Chen, 2018; Mao et al., 2024). However, it still outperforms most advanced methods with an average AUC-ROC of 0.84 (ranked 13th out of 29 methods; see Fig. 2A). PA performs better as the heterogeneity of node degrees increases. This out-performance is due to degree bias, where the positive edges are more likely to be formed by nodes with high degree and thereby are easily distinguishable from the negative edges. Thus, the current benchmark design favors methods that make predictions based largely on node degrees. This spurious performance of PA is evident when using Hits@K (Appendix E.6), indicating that the issue stems from the benchmark design rather than evaluation metrics. This spurious performance of PA also persists for larger-scale graphs (Appendix E.4).

## 2.5. Theoretical analysis

Many empirical graphs exhibit heterogeneous degree distributions, with a few nodes having exceptionally large degrees and most having small ones. These distributions are often characterized by power-law degree distribution  $p(k) \propto$

$k^{-\alpha}$  with  $\alpha \in (2, 3]$  (i.e., scale-free networks) (Albert & Barabási, 2002; Barabási & Bonabeau, 2003; Holme, 2019; Voitalov et al., 2019) or log-normal distributions (Broido & Clauset, 2019; Artico et al., 2020). While the power-law and log-normal distributions are both continuous, they are often used to approximate discrete degree distribution (Johnson et al., 1995; Redner, 2005; Radicchi et al., 2008; Clauset et al., 2009; Broido & Clauset, 2019; Artico et al., 2020). We show that the AUC-ROC for PA reaches near-maximum under log-normal distributions with heterogeneous node degrees. See Appendix E.3 for the case of power-law distributions.

Let us consider a general degree distribution  $p(k)$  without restricting ourselves to log-normal distributions. The AUC-ROC has a probabilistic interpretation (Hand, 2009): it is the probability that the score  $s^+$  for positive edges is larger than the score  $s^-$  for negative edges. Recalling that PA computes  $s_{ij} = k_i k_j$ , the AUC-ROC for PA is given by

$$\text{AUC-ROC} = P(s_{i^-, j^-} \leq s_{i^+, j^+}) = P(k_{i^-} k_{j^-} \leq k_{i^+} k_{j^+}), \quad (2)$$

where  $i^\pm$  and  $j^\pm$  represent the nodes of the positive and negative edges, respectively. We define the degree bias by Eq 2. The AUC-ROC represents the discrepancy between the distributions of the prediction scores  $k_{i^-} k_{j^-}$  for nega-

tive edges and the scores  $k_i + k_j$  for positive edges. If the positive edges have higher scores than the negative edges, the AUC-ROC approaches 1, indicating that node degree alone can effectively predict the positive edges. Conversely, if the positive and negative edges have similar scores, the AUC-ROC nears 0.5, indicating node degree alone is insufficient for the prediction.

Now, let us assume that  $p(k)$  follows the log-normal distribution,  $\text{LogNorm}(k \mid \mu, \sigma^2)$ , given by (Hand, 2009):

$$p(k) = \text{LogNorm}(k \mid \mu, \sigma^2) \\ = \frac{1}{\sqrt{2\pi}\sigma k} \exp\left[-\frac{(\ln k - \mu)^2}{2\sigma^2}\right], \quad (3)$$

where  $\mu$  and  $\sigma$  are the parameters of the log-normal distribution. The mean of the log-normal degree distribution is  $\langle k \rangle = \exp(\mu + \sigma^2/2)$  (Hand, 2009). By leveraging a unique characteristic of log-normal distributions, we obtain the AUC-ROC for PA analytically as follows. The detailed derivation is provided in Appendix B.

$$P(\ln s^- < \ln s^+) = \Phi(\sigma).$$

where  $\Phi$  is the cumulative distribution function for the standard normal distribution. We have assumed no degree assortativity in the graph, where  $P(k_i^+, k_j^+) = P(k_i)P(k_j)$ . Although empirical graphs often exhibit degree assortativity, our results indicate that it does not significantly impact the AUC-ROC (Appendix E.2).

Equation 4 suggests the key behavior of AUC-ROC for PA. The AUC-ROC for PA is an increasing function of the parameter  $\sigma$  of the log-normal distribution (Fig. 1C). The parameter  $\sigma$  of the log-normal distribution controls the spread of the distribution, with larger  $\sigma$  resulting in a more fat-tailed distribution. While our assumptions about the log-normal degree distribution and degree assortativity may not always align with real-world data, Eq. 4 still effectively captures the AUC-ROC behavior for PA (Fig. 1C). Further analysis of power-law distributions is described in Appendix E.3. We also identified a similar degree bias in a triplet sampling method (Rendle et al., 2009), which samples triplets  $(i, j, j')$  by sampling an edge  $(i, j)$  and then sampling a node  $j'$  uniformly at random (Appendix C).

This theoretical result highlights the significant issue with the current link prediction benchmark: a high benchmark performance can be achieved by only learning node degrees, posing the question of whether the link prediction benchmark is an effective objective of graph machine learning.

### 3. The degree-corrected link prediction benchmark

The link prediction benchmark yields biased evaluations due to mismatched degree distributions between positive

and negative edges, i.e.,  $p_{\text{neg}}(k) \neq p_{\text{pos}}(k)$ . To mitigate the mismatch, we introduce the *degree-corrected link prediction benchmark* that samples negative edges with the same degree bias as positive edges (See Algorithm 1 in Appendix). Specifically, we create a list of nodes where each node with degree  $k$  appears  $k$  times. Then, we sample negative edges by uniformly sampling two nodes from this list with replacement until the sampled node pairs are not connected and not in the test edge set. Crucially, nodes with degree  $k$  are  $k$  times more likely to be sampled than nodes with degree 1, mirroring the degree bias of the positive edges. Consequently, the positive and negative edges in the degree-corrected benchmark are indistinguishable based on node degrees. A Python package for the degree-corrected benchmark will be made available on GitHub.

#### 3.1. Comparison of the benchmark evaluations

We reevaluated the methods using the degree-corrected link prediction benchmark, maintaining the same parameters as in the original benchmark. The results show a significant drop in the performance of PA, with most methods having AUC-ROC scores close to 0.5 for most networks (Fig. 1E). We find qualitatively the same results when using the Hits@K score (Appendix E.6).

We note that our aim is not to completely eliminate degree as a predictive feature but rather to remove the bias introduced by negative edge sampling. The degree can remain a meaningful predictor after correction if it genuinely correlates with the likelihood of edges between nodes. ‘biokg\_drug’ marks this point well; it has the strongest rich-club structure of all graphs (including non-OGB graphs), where 94% of edges connect the top 10% highest-degree nodes. In other OGB graphs, this figure is below 27%. Even after correction, degree remains a meaningful predictor for biokg\_drug (AUC-ROC of 0.9) because high-degree nodes are inherently more likely to be connected in this graph.

The degree-corrected benchmark has some agreement with the original benchmark in terms of the ranking of the methods (Fig. 2A). For example, they rank GAT and LRW as top performers, while NB, SGTAdjNeu, and SGTAdjExp are consistently ranked lower. On the other hand, the degree-corrected benchmark ranks PA as the lowest performer, with its average AUC-ROC dropping from 0.83 to 0.54, placing it last out of 29 methods. Other methods such as LPI, GIN also experience a substantial drop in their rankings from 4nd to 12th and 10th to 21th, respectively (Fig. 2A). On the other hand, GCN, GraphSAGE, node2vec, DeepWalk, and EigenMap increase their rankings substantially (Fig. 2A). (See Appendix E.1 for the ranking of methods by HeaRT benchmark (Li et al., 2024a).)

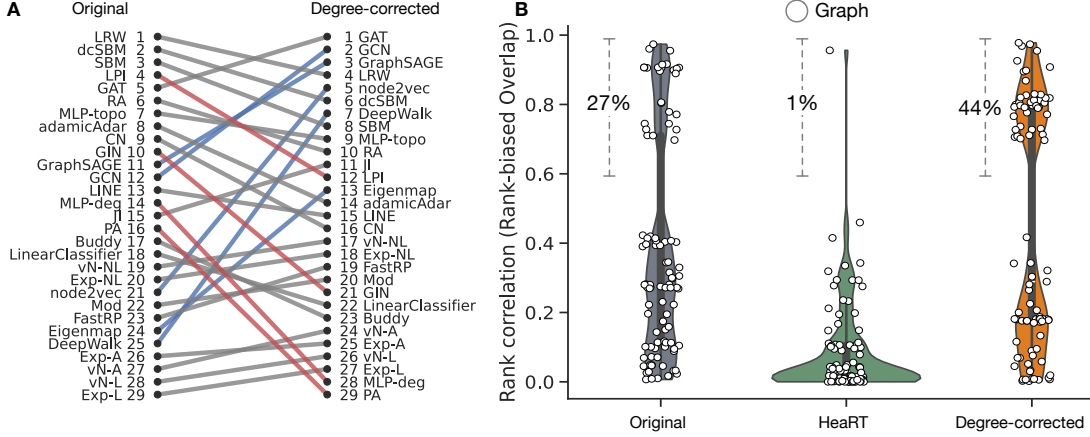


**Figure 2.** Comparative analysis of link prediction and recommendation benchmarks. **A:** Ranking changes for link prediction methods between original and degree-corrected benchmarks. Red and blue lines indicate methods with ranking shifts greater than 8 places. **B:** Ranking of methods by the degree-corrected benchmark is more aligned with that of the recommendation task than that of the original benchmark and the HeaRT benchmark. RBO (rank-biased overlap) measures the similarity between link prediction and recommendation task rankings.

### 3.2. The degree-corrected benchmark aligns better with recommendation tasks

Link prediction serves as a computationally efficient proxy for evaluating and training recommendation systems (Yang et al., 2015; Wang et al., 2021; Huang et al., 2023; Li et al., 2024a; Menand & Seshadri, 2024). In the recommendation task, directly optimizing recommendation metrics such as Hits@K requires ranking all possible node pairs for each node, which is computationally infeasible for large networks. In contrast, link prediction evaluates on a fixed set of candidate pairs, making it  $\mathcal{O}(M)$  (where  $M$  is the number of edges) and thus practical for both evaluation and training. This computational advantage has made link prediction benchmarks a de facto standard for developing and training recommendation models. However, this practice is only valid if link prediction performance correlates with recommendation performance. It is thus crucial that a link prediction benchmark accurately mirrors the performance in recommendation tasks.

Recommendation systems typically involve two steps: retrieval and ranking. First, the retriever selects a smaller candidate set from the entire node set, after which the ranker orders these candidates. In our experiments, we adopt a two-stage retrieval pipeline to reflect this practice. Initially, a retriever selects the top candidate neighbors per node using its similarity function. Then, a ranking model ranks these candidates. Both the retriever and the ranker are based on the same similarity function for the embedding- and topology-based models, but for pairwise link prediction models (i.e., BUDDY and MLP), we use the local random walk (LRW) to retrieve the candidate sets because enumer-

ating all node pairs is computationally challenging. We chose LRW because it is among the best performing methods in the retrieval task. The effectiveness of the recommendations is measured using the Normalized Discounted Cumulative Gain at  $K$  (NDCG@ $K$ ) (Järvelin & Kekäläinen, 2002). We perform this task five times and average the NDCG@ $K$  scores across different runs. We note that our results are consistent for different candidate set sizes (refer to Appendix E.5).

For each graph, we evaluate the alignment between the rankings based on the recommendation task and those based on the link prediction benchmarks using Rank Biased Overlap (RBO) (Webber et al., 2010). RBO is a ranking similarity metric with larger weights on the top performers in the two rankings. A larger RBO score indicates that the top performers in the two rankings are more similar. The weights on the top performer are controlled by the parameter  $p \in (0, 1)$ . While we set  $p = 0.5$  in our experiment, we confirmed that our results are robust to the choice of  $p$  (Appendix E.5).

Our results from 95 graphs show that the degree-corrected benchmark achieves higher RBO scores than the original benchmark. For reference, we also tested the HeaRT benchmark (Li et al., 2024a), which is a recent link prediction benchmark that mitigates the distance-based bias. The results show that HeaRT achieves substantially lower RBO scores than both the original and degree-corrected benchmarks. We find consistent results for different values of  $K$  and parameter  $p$  of the RBO (Appendix E.5). These results indicate that the degree-corrected benchmark more accurately mirrors the performance in recommendation tasks, providing a more reliable measure of the effectiveness of

methods in practical applications.

### 3.3. Degree-corrected benchmark facilitates the learning of community structure

The link prediction benchmark is a common unsupervised learning objective for GNNs (Tang et al., 2015; Hamilton et al., 2017; Kawamoto et al., 2018; Kojaku et al., 2021b). The degree bias implies that GNNs trained using the original link prediction benchmark tend to overfit to node degrees because they can easily differentiate between positive and negative edges based on node degrees. We show that the degree-corrected benchmark effectively prevents overfitting to node degrees and improves the learning of salient graph structures.

We evaluate GNNs on the common unsupervised task of community detection in graphs (Fortunato, 2010; Fortunato & Hric, 2016; Fortunato & Newman, 2022). The community detection task identifies densely connected groups (i.e., communities) in a graph. Community detection and link prediction tasks are intimately related (Clauset et al., 2008; Peixoto, 2018; Ghasemian et al., 2020). Two nodes will likely have edges if they belong to the same community. By training a graph machine learning model (e.g., GNNs) to learn a node embedding to predict links, nodes in the same community are mapped to be close to each other in the embedding space (Kojaku et al., 2024). Communities often correspond to functional units (e.g., social circles with similar opinions and protein complexes) in the graph, and detecting communities is a crucial task in many graph applications (Fortunato, 2010; Peixoto, 2013; Fortunato & Hric, 2016; Peixoto, 2018; Fortunato & Newman, 2022). Specifically, we test the GNNs by using the Lancichinetti-Fortunato-Radicchi (LFR) community detection benchmark (Lancichinetti et al., 2008), a standard benchmark for community detection (Fortunato, 2010; Fortunato & Hric, 2016; Tandon et al., 2021; Kojaku et al., 2024). The LFR benchmark generates synthetic graphs with predefined communities as follows. Each node  $i$  is assigned a degree  $k_i$  from a power-law distribution  $p(k) \sim k^{-\tau_1}$ , with maximum degree  $k_{\max}$ . A smaller  $\tau_1$  indicates a higher likelihood of large degree nodes, which results in a more heterogeneous degree distribution. Nodes are randomly grouped into  $L$  communities, with community sizes (i.e., the number of nodes in a community) following another power-law distribution  $p(n) \sim n^{-\tau_2}$  bounded between  $n_{\min}$  and  $n_{\max}$ . Edges are then formed such that each node  $i$  connects to a fraction  $1 - \mu$  of its  $k_i$  edges within its community and the remaining fraction  $\mu$  to nodes in other communities. We generate 10 graphs for  $\mu \in \{0.05, 0.1, 0.15, \dots, 0.95, 1\}$  using the following parameter values: the number of nodes  $N = 3,000$ , the degree exponent  $\tau_1 \in \{2.5, 3\}$ , the average degree  $\langle k \rangle = 25$ , the maximum degree  $k_{\max} = 1000$ , the community-size exponent  $\tau_2 = 3$ , the minimum and max-

imum community size  $n_{\min} = 100$  and  $n_{\max} = 1000$ . We obtained qualitatively similar results for different values of the parameters of the LFR benchmark (Appendix E.8).

We train GNNs using either the original or the degree-corrected link prediction benchmarks to minimize binary entropy loss in classifying the positive and negative edges. Using the trained GNNs, we generate node embeddings and apply the  $K$ -means clustering algorithm to detect communities, where  $K$  is set to the number of true communities. Although the number  $K$  of communities is often unknown, we use the ground-truth number to eliminate noise from estimating  $K$  and to concentrate on evaluating the quality of the learned node embeddings, a standard practice in benchmarking node embeddings for the community detection task (Tandon et al., 2021; Kojaku et al., 2024; Kovács et al., 2024). We measure the performance of GNNs by comparing the detected communities against the true communities using the adjusted element-centric similarity (Gates et al., 2019; Kojaku et al., 2024; Kovács et al., 2024), where higher scores indicate a higher similarity between the node partitions for the true and detected communities. We observe qualitatively similar results for partition similarities based on the normalized mutual information (Appendix E.7).

All GNNs, except for GIN, perform well when  $\mu \leq 0.5$ , where communities are distinct and easily identifiable, but their performance declines as  $\mu$  increases (Fig. 3A). Across a broad range of  $\mu$ , degree-corrected GNNs, particularly GIN, GCN, and GraphSAGE, outperform original GNNs in identifying communities, as shown by the area under the performance curve (Fig. 3B). The advantage of degree-corrected benchmarks becomes more evident with a more heterogeneous degree distribution (Fig. 3C and D). This indicates that degree correction effectively reduces overfitting to node degrees, enhancing the learning of community structures in graphs.

## 4. Discussion

We showed that common link prediction benchmarks are biased due to node degree in edge sampling, favoring methods that overfit to node degree. This bias distorts model evaluations and leads to suboptimal node embeddings (Fig. 2B, Fig. 3B). The degree bias we focused on is *artifactual*, i.e., it is not present in the actual network data but arises in the set of sampled positive and negative edges due to the biased sampling algorithm. We have shown that this artifactual bias significantly distorts the evaluation of link prediction models (Fig. 2B) and can be leveraged by these models to optimize their objective functions, leading to suboptimal learning of node embeddings (Fig. 3B).

To better understand the contribution of degree bias, we decomposed AUC-ROC scores into contributions from differ-

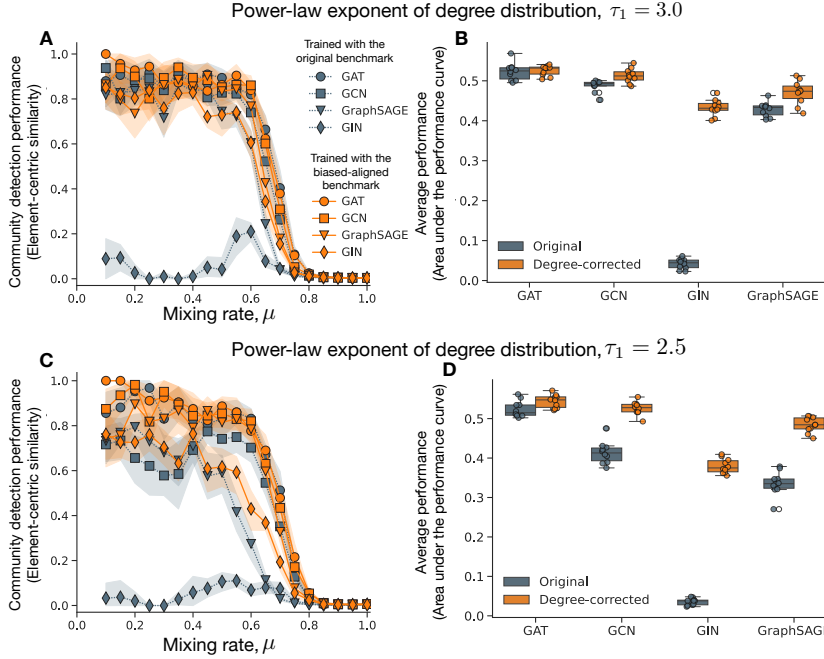


**Figure 3.** The degree-corrected benchmark improves GNNs in learning community structure in the LFR graphs. The graphs consist of 3,000 nodes with an average degree of 25. **A:** The performance of community detection for the LFR graphs with a power-law degree distribution with  $\tau_1 = 3.0$  as a function of mixing  $\mu$ . **B:** The average performance (by the area under the performance curve). **C, D:** The same plots for LFR graphs with a fatter power-law degree distribution with  $\tau_1 = 2.5$ . The error bars represent the 95% confidence interval estimated by a bootstrap of 1,000 repetitions.

ent node degree groups (Appendix D). Our analysis revealed that in networks with high degree heterogeneity ( $\sigma > 1.3$ ), a single combination—high-degree positive edges and low-degree negative edges—dominates the evaluation, accounting for over 80% of the overall AUC-ROC score. This finding explains why even simple degree-based methods perform well: the benchmark’s evaluation is largely determined by cases that can be easily classified using degree alone. Indeed, our logistic regression analysis shows that in heterogeneous networks, the degree product becomes overwhelmingly important, with its coefficient more than twice as large as other structural features (Appendix D). These results highlight how the sampling procedure inadvertently creates a shortcut that allows methods to achieve high performance without learning meaningful graph structures.

To address the degree bias, we proposed a degree-corrected benchmark that aligns the degree distributions of sampled edges. Our benchmark not only provided accurate evaluations but also improved GNN training by reducing overfitting to a degree and enhancing community detection.

While our focus is on degree bias, we acknowledge other biases identified by previous studies (Lichtnwalter & Chawla, 2012; Zhang & Chen, 2018; Mao et al., 2024; Li et al., 2024a). We highlight some of these biases to underscore the uniqueness of degree bias.

(1) Distance bias arises because nodes connected by negative edges are generally farther apart than those linked by positive edges (Li et al., 2024a), making them easily distinguishable by distance. We observed that correcting for degree bias consistently reduces distance bias; the degree-corrected benchmark showed more negative edges connected by paths of length 2 compared to the standard benchmark across all networks. While our degree correction naturally mitigates distance bias, distance debiasing does not address degree bias. This is evidenced by the strong performance of PA, a purely degree-based predictor, even after distance-bias correction (Appendix E.1). This asymmetry likely arises because node distances are inherently influenced by degree heterogeneity. In networks with high degree heterogeneity, high-degree nodes act as hubs, creating short paths between many node pairs. Correcting for degree bias naturally reduces the effect of these hub-mediated short paths. However, correcting for distance alone does not address the underlying degree heterogeneity, which continues to influence network structure and link prediction performance.

(2) Study (Huang et al., 2023) highlighted an issue arising from the substantial down-sampling of negative edges to match the number of positive edges. They proposed an “unbiased testing” approach for link prediction by evaluating methods on all possible negative pairs rather than just a sampled subset. However, we note that the concept of “bias”

in their work differs from the sampling bias we address. The degree bias we focus on stems from positive edge sampling, not negative edges. Sampling all negative edges does not resolve this degree bias at all because the node frequency in all negative edges still matches that of uniformly sampled negative edges.

(3) Our degree-corrected sampling may increase the frequency of high-degree nodes, but as these appear in negative examples, models are penalized for overfitting them. This encourages learning more nuanced features, improving the capture of network structures like communities (Fig. 3). This approach parallels techniques in stock market analysis (MacMahon & Garlaschelli, 2015), community detection (Newman, 2006), and node embedding (Kojaku et al., 2021b), where filtering dominant patterns reveals finer structural relationships.

In summary, our findings add a new direction to the ongoing examination of the link prediction task by demonstrating that node degree—a local and notably simpler attribute than distance—is often sufficient for differentiating the positive and negative edges. Crucially, the degree bias arises in any non-regular graph, regardless of the structure of the graph, because the bias stems not from the graph structure but from the *edge sampling algorithm* used in the link prediction benchmark. More broadly, edge sampling—the source of the degree bias—is a general technique for evaluating and training graph machine learning. For instance, mini-batch training (Hamilton et al., 2017; Hu et al., 2020b), which samples subsets of edges for efficient GNN training, may also exhibit bias due to node degrees, leading to skewed training sets. Given the widespread use of edge sampling across various graph machine-learning tasks, our findings have broad implications beyond link prediction benchmarks, extending to a range of benchmarks and training frameworks.

Our study has several limitations. First, we did not explore the reasons behind the varying performance of different link prediction methods. Degree heterogeneity can negatively impact GNNs (Liu et al., 2021; Kang et al., 2022; Subramonian et al., 2024b; Wang et al., 2024; Liu et al., 2023; Subramonian et al., 2024a; Arun et al., 2023; Li et al., 2024b). Small-degree nodes tend to have poor representation quality due to limited neighborhood information (Liu et al., 2021; Wang et al., 2024), and large-degree nodes benefit from reinforced structural inequality (Subramonian et al., 2024b; Liu et al., 2023; Li et al., 2024b). This—how well a method represents low-degree nodes—could be one reason for the differences in performance. It is important to note that there is no single link prediction method that is universally effective for all graphs because the performance of link prediction methods depends on the assumptions on the graph structure to make the predictions (Ghasemian et al., 2020). Second, we focus on community structure to test the effectiveness of the proposed benchmark as a training framework. However,

other non-trivial graph structures, such as centrality, could be tested through network dismantling benchmarks (Osat et al., 2023). Third, our degree correction method addresses one form of bias; it may potentially introduce new biases, although we could not identify any clear example of such biases. As a precaution, we investigated whether our debiasing method can exacerbate certain other biases identified in the literature, such as the distance bias Li et al. (2024a), and found no evidence of this. In fact, we find that our method mitigates the distance bias and not vice versa. Fourth, our analysis focuses on the transductive setting, where link prediction occurs between nodes in the training graph. We note that degree bias likely persists inductively since new nodes with more connections are still more likely to be selected in edge sampling, mirroring the bias in the transductive setting. Fourth, our study focuses exclusively on unipartite networks, and while the findings reveal meaningful insights about degree bias and benchmarking in this setting, their applicability to bipartite or heterogeneous graphs remains unclear and is an important avenue for future investigation.

Despite these limitations, our results suggest that sampling graph data is a highly non-trivial task more than the commonly considered. Because sampling edges from a graph is integral to evaluating and training graph machine learning methods, our results underline the importance of careful sampling to ensure the effectiveness of evaluations and training of graph machine learning methods.

## Software and Data

### 4.1. Source data and code

The source data, code, and workflow for our experiments are available on GitHub at <https://github.com/skojaku/degree-corrected-link-prediction-benchmark>.

## Acknowledgments

We acknowledge NVIDIA Corporation for their GPU resources and express our gratitude to Kaleb Smith from the NVIDIA SAE-Higher Education Research team for his help of GPU optimization. This work was supported by the Air Force Office of Scientific Research under Grant No. FA9550-19-1-0391 and FA9550-25-1-0087. J.Y. acknowledges Global Humanities and Social Sciences Convergence Research Program through the National Research Foundation of Korea (NRF), funded by the Ministry of Education (2024S1A5C3A02042671).

## Impact Statement

Our findings indicate that the standard benchmark promotes link prediction algorithms that enhance the “rich-get-richer”

effect, where well-connected nodes tend to gain even more connections. This effect, known as *preferential attachment*, is common in various societal contexts. For instance, popular individuals often gain more friends, widely shared content spreads further, and frequently cited papers are more likely to attract additional citations. While preferential attachment can benefit distributing resources and recognition, it also presents significant disadvantages. For example, preferential attachment can disproportionately favor well-connected individuals in professional networks and hinder scientific progress by undervaluing innovative papers from less-known researchers (Chu & Evans, 2021). Our analysis indicates that the recommendation algorithms trained using the existing benchmark may exacerbate social inequalities by reinforcing the preferential attachment mechanism. Our new benchmark directly addresses these concerns by negating the degree bias, promoting fairer algorithm evaluations, and supporting the development of fairness-aware machine learning methods.

## References

- Graph-Tool: Efficient Network Analysis with Python. <https://graph-tool.skewed.de/>.
- GitHub changyaochen/rbo. <https://github.com/changyaochen/rbo>. [Accessed 26-Apr-2024].
- Abbas, K., Abbasi, A., Dong, S., Niu, L., Yu, L., Chen, B., Cai, S.-M., and Hasan, Q. Application of network link prediction in drug discovery. *BMC Bioinformatics*, 22:1–21, 2021.
- Abboud, R., Ceylan, I. I., Grohe, M., and Lukasiewicz, T. The Surprising Power of Graph Neural Networks with Random Node Initialization. In *International Joint Conference on Artificial Intelligence*, 2020. URL <https://api.semanticscholar.org/CorpusID:222134198>.
- Abraham, L. fastnode2vec, 2020. URL <https://github.com/louisabraham/fastnode2vec>.
- Adamic, L. A. and Adar, E. Friends and neighbors on the web. *Social Networks*, 25(3):211–230, 2003.
- Albert, R. and Barabási, A.-L. Statistical mechanics of complex networks. *Reviews of modern physics*, 74(1):47, 2002.
- Ali, M., Hoyt, C. T., Domingo-Fernández, D., Lehmann, J., and Jabeen, H. BioKEEN: a library for learning and evaluating biological knowledge graph embeddings. *Bioinformatics*, 35(18):3538–3540, 2019.
- Alstott, J., Bullmore, E., and Plenz, D. powerlaw: a Python package for analysis of heavy-tailed distributions. *PloS ONE*, 9(1):e85777, 2014.
- Artico, I., Smolyarenko, I., Vinciotti, V., and Wit, E. C. How rare are power-law networks really? *Proceedings of the Royal Society A*, 476(2241):20190742, 2020.
- Arun, A., Aanegola, A., Agrawal, A., Narayanan, R., and Kumaraguru, P. CAFIN: Centrality Aware Fairness Inducing IN-Processing for Unsupervised Representation Learning on Graphs. In *ECAI 2023*, pp. 101–108. IOS Press, 2023.
- Barabási, A.-L. and Bonabeau, E. Scale-free networks. *Scientific american*, 288(5):60–69, 2003.
- Barabási, A.-L. and Pósfai, M. *Network Science*. Cambridge University Press, Cambridge, United Kingdom, 1st edition edition, 2016. ISBN 978-1-107-07626-6.
- Barthélemy, M., Barrat, A., Pastor-Satorras, R., and Vespignani, A. Velocity and hierarchical spread of epidemic outbreaks in scale-free networks. *Physical Review letters*, 92(17):178701, 2004.
- Belkin, M. and Niyogi, P. Laplacian Eigenmaps for Dimensionality Reduction and Data Representation. *Neural Computation*, 15(6):1373–1396, 2003. ISSN 0899-7667.
- Bishop, C. M. Pattern recognition and machine learning. *Springer google schola*, 2:1122–1128, 2006.
- Bordes, A., Usunier, N., Garcia-Duran, A., Weston, J., and Yakhnenko, O. Translating embeddings for modeling multi-relational data. *Advances in Neural Information Processing Systems*, 26, 2013.
- Breit, A., Ott, S., Agibetov, A., and Samwald, M. Open-BioLink: a benchmarking framework for large-scale biomedical link prediction. *Bioinformatics*, 36(13):4097–4098, 2020.
- Broido, A. D. and Clauset, A. Scale-free networks are rare. *Nature communications*, 10(1):1017, 2019.
- Cai, L., Li, J., Wang, J., and Ji, S. Line graph neural networks for link prediction. *IEEE Transactions on Pattern Analysis and Machine Intelligence*, 44(9):5103–5113, 2021.
- Chamberlain, B. P., Shirobokov, S., Rossi, E., Frasca, F., Markovich, T., Hammerla, N. Y., Bronstein, M. M., and Hansmire, M. Graph Neural Networks for Link Prediction with Subgraph Sketching. In *The Eleventh International Conference on Learning Representations*, 2023. URL <https://openreview.net/forum?id=mloqEOAozQU>.
- Chen, H., Sultan, S. F., Tian, Y., Chen, M., and Skiena, S. Fast and accurate network embeddings via very sparse random projection. In *Proceedings of the 28th ACM*

- International Conference on information and knowledge management*, pp. 399–408, 2019.
- Christakis, N. A. and Fowler, J. H. Social network sensors for early detection of contagious outbreaks. *Plos ONE*, 5(9):e12948, 2010.
- Chu, J. S. and Evans, J. A. Slowed canonical progress in large fields of science. *Proceedings of the National Academy of Sciences*, 118(41):e2021636118, 2021.
- Clauset, A., Moore, C., and Newman, M. E. Hierarchical structure and the prediction of missing links in networks. *Nature*, 453(7191):98–101, 2008.
- Clauset, A., Shalizi, C. R., and Newman, M. E. Power-law distributions in empirical data. *SIAM review*, 51(4):661–703, 2009.
- Crichton, G., Guo, Y., Pyysalo, S., and Korhonen, A. Neural networks for link prediction in realistic biomedical graphs: a multi-dimensional evaluation of graph embedding-based approaches. *BMC Bioinformatics*, 19:1–11, 2018.
- Deng, J., Dong, W., Socher, R., Li, L.-J., Li, K., and Fei-Fei, L. Imagenet: A large-scale hierarchical image database. In *2009 IEEE conference on computer vision and pattern recognition*, pp. 248–255. IEEE, 2009.
- Erkol, S., Castellano, C., and Radicchi, F. Systematic comparison between methods for the detection of influential spreaders in complex networks. *Scientific Reports*, 9(1):15095, 2019.
- Feld, S. L. Why your friends have more friends than you do. *American journal of sociology*, 96(6):1464–1477, 1991.
- Fey, M. and Lenssen, J. E. Fast Graph Representation Learning with PyTorch Geometric. In *ICLR Workshop on Representation Learning on Graphs and Manifolds*, 2019.
- Fortunato, S. Community Detection in Graphs. *Physics Reports*, 486(3):75–174, 2010. ISSN 0370-1573.
- Fortunato, S. and Hric, D. Community Detection in Networks: A User Guide. *Physics Reports*, 659:1–44, 2016. ISSN 0370-1573.
- Fortunato, S. and Newman, M. E. J. 20 Years of Network Community Detection. *Nature Physics*, 18(8):848–850, 2022. ISSN 1745-2481.
- Gates, A. J., Wood, I. B., Hetrick, W. P., and Ahn, Y.-Y. Element-Centric Clustering Comparison Unifies Overlaps and Hierarchy. *Scientific Reports*, 9(1):8574, 2019. ISSN 2045-2322.
- Ghasemian, A., HosseiniMardi, H., Galstyan, A., Airoldi, E. M., and Clauset, A. Stacking models for nearly optimal link prediction in complex networks. *Proceedings of the National Academy of Sciences*, 117(38):23393–23400, 2020.
- Goyal, P. and Ferrara, E. Graph embedding techniques, applications, and performance: A survey. *Knowledge-Based Systems*, 151:78–94, 2018.
- Grover, A. and Leskovec, J. Node2vec: Scalable Feature Learning for Networks. In *Proceedings of the 22nd ACM SIGKDD International Conference on KDD*, KDD ’16, pp. 855–864, New York, NY, USA, 2016. Association for Computing Machinery. ISBN 978-1-4503-4232-2.
- Hamilton, W., Ying, Z., and Leskovec, J. Inductive representation learning on large graphs. *Advances in Neural Information Processing Systems*, 30, 2017.
- Hand, D. J. Measuring classifier performance: a coherent alternative to the area under the ROC curve. *Machine learning*, 77(1):103–123, 2009.
- He, X., Ghasemian, A., Lee, E., Schwarze, A. C., Clauset, A., and Mucha, P. J. Link prediction accuracy on real-world networks under non-uniform missing-edge patterns. *Plos one*, 19(7):e0306883, 2024.
- Holme, P. Rare and everywhere: Perspectives on scale-free networks. *Nature communications*, 10(1):1016, 2019.
- Hu, W., Fey, M., Zitnik, M., Dong, Y., Ren, H., Liu, B., Catasta, M., and Leskovec, J. Open graph benchmark: Datasets for machine learning on graphs. *Advances in neural information processing systems*, 33:22118–22133, 2020a.
- Hu, Z., Dong, Y., Wang, K., and Sun, Y. Heterogeneous graph transformer. In *Proceedings of the Web Conference 2020*, pp. 2704–2710, 2020b.
- Huang, Z., Li, X., and Chen, H. Link prediction approach to collaborative filtering. In *Proceedings of the 5th ACM/IEEE-CS joint conference on Digital libraries*, pp. 141–142, 2005.
- Huang, Z., Kosan, M., Silva, A., and Singh, A. Link prediction without graph neural networks. *arXiv preprint arXiv:2305.13656*, 2023.
- Ito, T., Shimbo, M., Kudo, T., and Matsumoto, Y. Application of kernels to link analysis. In *Proceedings of the eleventh ACM SIGKDD International Conference on Knowledge discovery in data mining*, pp. 586–592, 2005.
- Jacob, R., Harikrishnan, K., Misra, R., and Ambika, G. Measure for degree heterogeneity in complex networks

- and its application to recurrence network analysis. *Royal Society open science*, 4(1):160757, 2017.
- Järvelin, K. and Kekäläinen, J. Cumulated gain-based evaluation of IR techniques. *ACM Transactions on Information Systems (TOIS)*, 20(4):422–446, 2002.
- Johnson, N. L., Kotz, S., and Balakrishnan, N. *Continuous univariate distributions, volume 2*, volume 289. John wiley & sons, 1995.
- Kang, J., Zhu, Y., Xia, Y., Luo, J., and Tong, H. Rawlsgcn: Towards rawlsian difference principle on graph convolutional network. In *Proceedings of the ACM Web Conference 2022*, pp. 1214–1225, 2022.
- Karrer, B. and Newman, M. E. J. Stochastic Blockmodels and Community Structure in Networks. *Physical Review E*, 83(1):016107, 2011.
- Kawamoto, T., Tsubaki, M., and Obuchi, T. Mean-field theory of graph neural networks in graph partitioning. *Advances in Neural Information Processing Systems*, 31, 2018.
- Kipf, T. N. and Welling, M. Semi-Supervised Classification with Graph Convolutional Networks. In *International Conference on Learning Representations (ICLR)*, 2017.
- Kojaku, S., Hébert-Dufresne, L., Mones, E., Lehmann, S., and Ahn, Y.-Y. The Effectiveness of Backward Contact Tracing in Networks. *Nature Physics*, 17(5):652–658, 2021a. ISSN 1745-2481.
- Kojaku, S., Yoon, J., Constantino, I., and Ahn, Y.-Y. Residual2Vec: Debiasing graph embedding with random graphs. *Advances in Neural Information Processing Systems*, 34:24150–24163, 2021b.
- Kojaku, S., Radicchi, F., Ahn, Y.-Y., and Fortunato, S. Network community detection via neural embeddings. *Nature Communications*, 15(1):9446, 2024.
- Kondor, R. I. and Lafferty, J. Diffusion kernels on graphs and other discrete structures. In *Proceedings of the 19th International Conference on Machine Learning*, volume 2002, pp. 315–322, 2002.
- Kovács, B., Kojaku, S., Palla, G., and Fortunato, S. Iterative embedding and reweighting of complex networks reveals community structure. *Scientific Reports*, 14(1):17184, 2024.
- Krizhevsky, A., Sutskever, I., and Hinton, G. E. Imagenet classification with deep convolutional neural networks. *Advances in Neural Information Processing Systems*, 25, 2012.
- Krzakala, F., Moore, C., Mossel, E., Neeman, J., Sly, A., Zdeborová, L., and Zhang, P. Spectral Redemption in Clustering Sparse Networks. *Proceedings of the National Academy of Sciences*, 110(52):20935–20940, 2013.
- Kunegis, J. and Lommatzsch, A. Learning spectral graph transformations for link prediction. In *Proceedings of the 26th Annual International Conference on Machine Learning*, pp. 561–568, 2009.
- Lancichinetti, A. and Fortunato, S. Community detection algorithms: a comparative analysis. *Physical Review E*, 80(5):056117, 2009.
- Lancichinetti, A., Fortunato, S., and Radicchi, F. Benchmark Graphs for Testing Community Detection Algorithms. *Physical Review E*, 78(4):046110, 2008.
- Li, J., Shomer, H., Mao, H., Zeng, S., Ma, Y., Shah, N., Tang, J., and Yin, D. Evaluating graph neural networks for link prediction: Current pitfalls and new benchmarking. *Advances in Neural Information Processing Systems*, 36, 2024a.
- Li, Y., Yang, Y., Cao, J., Liu, S., Tang, H., and Xu, G. Toward Structure Fairness in Dynamic Graph Embedding: A Trend-aware Dual Debiasing Approach. In *Proceedings of the 30th ACM SIGKDD Conference on Knowledge Discovery and Data Mining*, pp. 1701–1712, 2024b.
- Liben-Nowell, D. and Kleinberg, J. The Link Prediction Problem for Social Networks. In *Proceedings of the Twelfth International Conference on Information and Knowledge Management, CIKM '03*, pp. 556–559, New York, NY, USA, 2003. Association for Computing Machinery. ISBN 1581137230. doi: 10.1145/956863.956972. URL <https://doi.org/10.1145/956863.956972>.
- Lichtnwalter, R. and Chawla, N. V. Link prediction: fair and effective evaluation. In *2012 IEEE/ACM International Conference on Advances in Social Networks Analysis and Mining*, pp. 376–383. IEEE, 2012.
- Lin, Z., Yin, Y., Liu, L., and Wang, D. SciSciNet: A large-scale open data lake for the science of science research. *Scientific Data*, 10(1):315, 2023.
- Liu, W. and Lü, L. Link prediction based on local random walk. *Europhysics Letters*, 89(5):58007, 2010.
- Liu, Z., Nguyen, T.-K., and Fang, Y. Tail-GNN: Tail-Node Graph Neural Networks. In *Proceedings of the 27th ACM SIGKDD Conference on Knowledge Discovery & Data Mining, KDD '21*, pp. 1109–1119, New York, NY, USA, 2021. Association for Computing Machinery. ISBN 9781450383325. doi: 10.1145/3447548.3467276. URL <https://doi.org/10.1145/3447548.3467276>.

- Liu, Z., Nguyen, T.-K., and Fang, Y. On generalized degree fairness in graph neural networks. In *Proceedings of the AAAI Conference on Artificial Intelligence*, volume 37, pp. 4525–4533, 2023.
- Lü, L., Jin, C.-H., and Zhou, T. Similarity index based on local paths for link prediction of complex networks. *Phys. Rev. E*, 80:046122, Oct 2009. doi: 10.1103/PhysRevE.80.046122. URL <https://link.aps.org/doi/10.1103/PhysRevE.80.046122>.
- MacMahon, M. and Garlaschelli, D. Community Detection for Correlation Matrices. *Phys. Rev. X*, 5:021006, Apr 2015. doi: 10.1103/PhysRevX.5.021006. URL <https://link.aps.org/doi/10.1103/PhysRevX.5.021006>.
- Mao, H., Li, J., Shomer, H., Li, B., Fan, W., Ma, Y., Zhao, T., Shah, N., and Tang, J. Revisiting Link Prediction: a data perspective. In *The Twelfth International Conference on Learning Representations*, 2024. URL <https://openreview.net/forum?id=8Ur2xmuw7w>.
- Mara, A. C., Lijffijt, J., and De Bie, T. Benchmarking network embedding models for link prediction: Are we making progress? In *2020 IEEE 7th International conference on data science and advanced analytics (DSAA)*, pp. 138–147. IEEE, 2020.
- Mason, S. J. and Graham, N. E. Areas beneath the relative operating characteristics (ROC) and relative operating levels (ROL) curves: Statistical significance and interpretation. *Quarterly Journal of the Royal Meteorological Society: A Journal of the Atmospheric Sciences, Applied Meteorology and Physical Oceanography*, 128 (584):2145–2166, 2002.
- Menand, N. and Seshadhri, C. Link prediction using low-dimensional node embeddings: The measurement problem. *Proceedings of the National Academy of Sciences*, 121(8):e2312527121, 2024.
- Menon, A. K. and Elkan, C. Link prediction via matrix factorization. In *Machine Learning and Knowledge Discovery in Databases: European Conference, ECML PKDD 2011, Athens, Greece, September 5-9, 2011, Proceedings, Part II* 22, pp. 437–452. Springer, 2011.
- Nadakuditi, R. R. and Newman, M. E. J. Graph Spectra and the Detectability of Community Structure in Networks. *Physical Review Letters*, 108(18):188701, 2012.
- Narayanan, A., Shi, E., and Rubinstein, B. I. Link prediction by de-anonymization: How we won the kaggle social network challenge. In *The 2011 International Joint Conference on Neural Networks*, pp. 1825–1834. IEEE, 2011.
- Newman, M. E. Modularity and community structure in networks. *Proceedings of the national academy of sciences*, 103(23):8577–8582, 2006.
- Newman, M. E. Network structure from rich but noisy data. *Nature Physics*, 14(6):542–545, 2018.
- Osat, S., Papadopoulos, F., Teixeira, A. S., and Radicchi, F. Embedding-aided network dismantling. *Physical Review Research*, 5(1):013076, 2023.
- Ou, M., Cui, P., Pei, J., Zhang, Z., and Zhu, W. Asymmetric transitivity preserving graph embedding. In *Proceedings of the 22nd ACM SIGKDD International Conference on Knowledge discovery and data mining*, pp. 1105–1114, 2016.
- Patent, U. S. and Office, T. USPTO citation network. 2023.
- Pedregosa, F., Varoquaux, G., Gramfort, A., Michel, V., Thirion, B., Grisel, O., Blondel, M., Prettenhofer, P., Weiss, R., Dubourg, V., Vanderplas, J., Passos, A., Cournapeau, D., Brucher, M., Perrot, M., and Duchesnay, E. Scikit-learn: Machine Learning in Python. *Journal of Machine Learning Research*, 12:2825–2830, 2011.
- Peixoto, T. P. Parsimonious Module Inference in Large Networks. *Physical Review Letters*, 110(14):148701, 2013.
- Peixoto, T. P. Reconstructing networks with unknown and heterogeneous errors. *Physical Review X*, 8(4):041011, 2018.
- Peixoto, T. P. The Netzschleuder network catalogue and repository. URL <https://networks.skewed.de>, 2020.
- Perozzi, B., Al-Rfou, R., and Skiena, S. DeepWalk: Online Learning of Social Representations. In *Proceedings of the 20th ACM SIGKDD International Conference on KDD*, KDD ’14, pp. 701–710, New York, NY, USA, 2014. Association for Computing Machinery. ISBN 978-1-4503-2956-9.
- Radicchi, F., Fortunato, S., and Castellano, C. Universality of citation distributions: Toward an objective measure of scientific impact. *Proceedings of the National Academy of Sciences*, 105(45):17268–17272, 2008.
- Rajpurkar, P., Zhang, J., Lopyrev, K., and Liang, P. SQuAD: 100,000+ Questions for Machine Comprehension of Text. In Su, J., Duh, K., and Carreras, X. (eds.), *Proceedings of the 2016 Conference on Empirical Methods in Natural Language Processing*, pp. 2383–2392, Austin, Texas, November 2016. Association for Computational Linguistics. doi: 10.18653/v1/D16-1264. URL <https://aclanthology.org/D16-1264>.

- Rajpurkar, P., Jia, R., and Liang, P. Know What You Don't Know: Unanswerable Questions for SQuAD. In Gurevych, I. and Miyao, Y. (eds.), *Proceedings of the 56th Annual Meeting of the Association for Computational Linguistics (Volume 2: Short Papers)*, pp. 784–789, Melbourne, Australia, July 2018. Association for Computational Linguistics. doi: 10.18653/v1/P18-2124. URL <https://aclanthology.org/P18-2124>.
- Redner, S. Citation statistics from 110 years of physical review. *Physics today*, 58(6):49–54, 2005.
- Rehurek, R. and Sojka, P. Gensim—python framework for vector space modelling. *NLP Centre, Masaryk University, Czech Republic*, 3(2), 2011.
- Rendle, S., Freudenthaler, C., Gantner, Z., and Schmidt-Thieme, L. BPR: Bayesian Personalized Ranking from Implicit Feedback. *ArXiv*, abs/1205.2618, 2009. URL <https://api.semanticscholar.org/CorpusID:10795036>.
- Russo, M., Sawischa, S. F., and Vidal, M.-E. Tracing the Impact of Bias in Link Prediction. In *Proceedings of the 39th ACM/SIGAPP Symposium on Applied Computing*, SAC '24, pp. 1626–1633, New York, NY, USA, 2024. Association for Computing Machinery. ISBN 9798400702433. doi: 10.1145/3605098.3635912. URL <https://doi.org/10.1145/3605098.3635912>.
- Sato, R., Yamada, M., and Kashima, H. Random features strengthen graph neural networks. In *Proceedings of the 2021 SIAM International Conference on data mining (SDM)*, pp. 333–341. SIAM, 2021.
- Subramonian, A., Kang, J., and Sun, Y. Theoretical and Empirical Insights into the Origins of Degree Bias in Graph Neural Networks. In *The Thirty-eighth Annual Conference on Neural Information Processing Systems*, 2024a. URL <https://openreview.net/forum?id=1mAaewThcz>.
- Subramonian, A., Sagun, L., and Sun, Y. Networked inequality: preferential attachment bias in graph neural network link prediction. In *Proceedings of the 41st International Conference on Machine Learning*, ICML'24. JMLR.org, 2024b.
- Sun, Z., Deng, Z.-H., Nie, J.-Y., and Tang, J. RotatE: Knowledge Graph Embedding by Relational Rotation in Complex Space. In *International Conference on Learning Representations*, 2019. URL <https://openreview.net/forum?id=HkgEQnRqYQ>.
- Tandon, A., Albeshri, A., Thayananthan, V., Alhalabi, W., Radicchi, F., and Fortunato, S. Community Detection in Networks Using Graph Embeddings. *Physical Review E*, 103(2):022316, 2021.
- Tang, J., Qu, M., Wang, M., Zhang, M., Yan, J., and Mei, Q. LINE: Large-scale Information Network Embedding. In *Proceedings of the 24th International Conference on World Wide Web*, WWW '15, pp. 1067–1077, Republic and Canton of Geneva, CHE, 2015. International World Wide Web Conferences Steering Committee. ISBN 978-1-4503-3469-3.
- Veličković, P., Cucurull, G., Casanova, A., Romero, A., Liò, P., and Bengio, Y. Graph Attention Networks. *International Conference on Learning Representations*, 2018. URL <https://openreview.net/forum?id=rJXMpikCZ>. accepted as poster.
- Virtanen, P., Gommers, R., Oliphant, T. E., Haberland, M., Reddy, T., Cournapeau, D., Burovski, E., Peterson, P., Weckesser, W., Bright, J., van der Walt, S. J., Brett, M., Wilson, J., Millman, K. J., Mayorov, N., Nelson, A. R. J., Jones, E., Kern, R., Larson, E., Carey, C. J., Polat, İ., Feng, Y., Moore, E. W., VanderPlas, J., Laxalde, D., Perktold, J., Cimrman, R., Henriksen, I., Quintero, E. A., Harris, C. R., Archibald, A. M., Ribeiro, A. H., Pedregosa, F., van Mulbregt, P., and SciPy 1.0 Contributors. SciPy 1.0: Fundamental Algorithms for Scientific Computing in Python. *Nature Methods*, 17:261–272, 2020.
- Voitalov, I., Van Der Hoorn, P., Van Der Hofstad, R., and Krioukov, D. Scale-free networks well done. *Physical Review Research*, 1(3):033034, 2019.
- Wang, P., Xu, B., Wu, Y., and Zhou, X. Link prediction in social networks: the state-of-the-art. *Science China Information Sciences*, pp. 1–38, 2014.
- Wang, S.-M., Lee, H.-K., Kweon, Y.-S., Lee, C. T., and Lee, K.-U. Overactive bladder successfully treated with duloxetine in a female adolescent. *Clinical Psychopharmacology and Neuroscience*, 13(2):212, 2015.
- Wang, Y. and Derr, T. Degree-Related Bias in Link Prediction. In *2022 IEEE International Conference on Data Mining Workshops (ICDMW)*, pp. 757–758, 2022. doi: 10.1109/ICDMW58026.2022.00103.
- Wang, Y., Zhao, T., Zhao, Y., Liu, Y., Cheng, X., Shah, N., and Derr, T. A Topological Perspective on Demystifying GNN-Based Link Prediction Performance. In *The Twelfth International Conference on Learning Representations*, 2024. URL <https://openreview.net/forum?id=apA6SSXx2e>.
- Wang, Z., Zhou, Y., Hong, L., Zou, Y., Su, H., and Chen, S. Pairwise learning for neural link prediction. *arXiv preprint arXiv:2112.02936*, 2021.
- Webber, W., Moffat, A., and Zobel, J. A Similarity Measure for Indefinite Rankings. *ACM Trans. Inf.*

*Syst.*, 28(4), nov 2010. ISSN 1046-8188. doi: 10.1145/1852102.1852106. URL <https://doi.org/10.1145/1852102.1852106>.

Xu, K., Hu, W., Leskovec, J., and Jegelka, S. How Powerful are Graph Neural Networks? In *International Conference on Learning Representations*, 2019. URL <https://openreview.net/forum?id=ryGs6iA5Km>.

Yang, Y., Lichtenwalter, R. N., and Chawla, N. V. Evaluating link prediction methods. *Knowledge and Information Systems*, 45:751–782, 2015.

You, J., McLeod, R. D., and Hu, P. Predicting drug-target interaction network using deep learning model. *Computational biology and chemistry*, 80:90–101, 2019.

Yue, X., Wang, Z., Huang, J., Parthasarathy, S., Moosavinasab, S., Huang, Y., Lin, S. M., Zhang, W., Zhang, P., and Sun, H. Graph embedding on biomedical networks: methods, applications and evaluations. *Bioinformatics*, 36(4):1241–1251, 2020.

Zhang, M. and Chen, Y. Link prediction based on graph neural networks. *Advances in Neural Information Processing Systems*, 31, 2018.

Zhou, T., Ren, J., Medo, M., and Zhang, Y.-C. Bipartite network projection and personal recommendation. *Physical Review E*, 76(4):046115, 2007.

Zhou, T., Lü, L., and Zhang, Y.-C. Predicting missing links via local information. *The European Physical Journal B*, 71:623–630, 2009.

## A. Data and link prediction methods

### A.1. Network data

The corpus of networks used in this work comprises networks with the number of nodes in the range  $[10^2, 10^6]$  and edges in the range  $[10^2, 10^8]$ . We also considered networks from the OGB benchmark (Hu et al., 2020a). This includes social, technological, information, biological, and transportation (spatial) networks. For simplicity in our analysis, we consider these networks to be unweighted, undirected, and without self-loops, though the message of our work holds without these constraints. The largest networks in our corpus (number of nodes  $> 10^5$ ) are sourced from Netzscheleuder (Peixoto, 2020), and the remaining networks are obtained from the authors of Ref. (Erkola et al., 2019). See Table 2 for details.

### A.2. Link prediction algorithms

We use 29 link prediction algorithms categorized into four groups: topology-based, graph embedding, network model, and graph neural networks (see Table 1).

#### A.2.1. TOPOLOGY-BASED PREDICTORS

Topology-based predictors calculate the prediction score  $s_{ij}$  using the structural features of two nodes. The topology-based predictors employed in our study include Preferential Attachment (PA) (Barabási & Pósfai, 2016), Common Neighbors (CN) (Liben-Nowell & Kleinberg, 2003), Adamic-Adar (AA) (Adamic & Adar, 2003), Jaccard Index (JI) (Liben-Nowell & Kleinberg, 2003), Resource Allocation (RA) (Zhou et al., 2007; 2009), Local Random Walk (LRW) (Liu & Lü, 2010), Local Path Index (LPI) (Lü et al., 2009). For LRW and LPI, we set the hyperparameter  $\epsilon = 0.001$  as per previous studies (Lü et al., 2009; Liu & Lü, 2010). The other methods do not require hyperparameters.

We implemented two multilayer perceptrons (MLPs) that takes features of two nodes and predict whether they are connected by an edge or not. The first MLP (MLP-deg) takes only the degree features as input, i.g., degree product  $k_i k_j$ , degree sum  $k_i + k_j$ , minimum degree  $\min(k_i, k_j)$ , and maximum degree  $\max(k_i, k_j)$ . The second MLP (MLP-topo) takes AA, JI, RA, and LRW as input. The MLP consists of two hidden layers coupled with a LeakyReLU activation function, and we used held-out validation to tune the number of dimensions in each hidden layer (32, 64) and dropout rate (0.2, 0.5) with the validation set consisting of 10% of the edges. We used the Adam optimizer at a learning rate of 0.001.

As a simpler baseline, we also implemented a logistic regression model (Linear) that takes the concatenation of the node features as input and predict whether they are connected by an edge or not. The input features are RA, JI, and LRW, and AA, and PA. In order to reduce the collinearity between the input features, we performed feature orthogonalization by regressing RA, JI, and LRW, AA on PA and taking the residuals as new features. This means that after orthogonalization, we input the residuals of RA, JI, and LRW, AA on PA, as well as the raw PA features to the logistic regression model. To further reduce the collinearity, we employed the ridge regression implemented in scikit-learn (Pedregosa et al., 2011), with the regularization parameter set to the default value.

#### A.2.2. GRAPH EMBEDDINGS

Graph embedding maps a graph into a vector space, with each node  $i$  represented by a point in this space. The prediction score  $s_{ij}$  is given by the dot product  $\vec{u}_i^\top \vec{u}_j$  between any two node vectors. We tested a variety of graph embedding methods including Laplacian EigenMap (EigenMap) (Belkin & Niyogi, 2003), Spectral Modularity (Mod) (Nadakuditi & Newman, 2012), Non-backtracking Embedding (NB) (Krzakala et al., 2013), FastRP (FastRP) (Chen et al., 2019), Exponential Kernel on Adjacency Matrix (Exp-A) (Kondor & Lafferty, 2002; Kunegis & Lommatzsch, 2009), Exponential Kernel on Laplacian (Exp-L) (Kondor & Lafferty, 2002; Kunegis & Lommatzsch, 2009), Exponential Kernel on Normalized Laplacian (Exp-NL) (Kondor & Lafferty, 2002; Kunegis & Lommatzsch, 2009), Von Neumann Kernel on Adjacency Matrix (vN-A) (Ito et al., 2005; Kunegis & Lommatzsch, 2009), Von Neumann Kernel on Laplacian (vN-L) (Ito et al., 2005; Kunegis & Lommatzsch, 2009), and Von Neumann Kernel on Normalized Laplacian (vN-NL) (Ito et al., 2005; Kunegis & Lommatzsch, 2009), node2vec (node2vec) (Grover & Leskovec, 2016), DeepWalk (DeepWalk) (Perozzi et al., 2014), and LINE (LINE) (Tang et al., 2015). We tested a variety of graph embedding methods including Laplacian EigenMap (EigenMap) (Belkin & Niyogi, 2003), Spectral Modularity (Mod) (Nadakuditi & Newman, 2012), Non-backtracking Embedding (NB) (Krzakala et al., 2013), FastRP (FastRP) (Chen et al., 2019), Exponential Kernel on Adjacency Matrix (Exp-A) (Kondor & Lafferty, 2002; Kunegis & Lommatzsch, 2009), Exponential Kernel on Laplacian (Exp-L) (Kondor & Lafferty, 2002; Kunegis & Lommatzsch, 2009), Exponential Kernel on Normalized Laplacian (Exp-NL) (Kondor &

Lafferty, 2002; Kunegis & Lommatzsch, 2009), Von Neumann Kernel on Adjacency Matrix (vN-A) (Ito et al., 2005; Kunegis & Lommatzsch, 2009), Von Neumann Kernel on Laplacian (vN-L) (Ito et al., 2005; Kunegis & Lommatzsch, 2009), and Von Neumann Kernel on Normalized Laplacian (vN-NL) (Ito et al., 2005; Kunegis & Lommatzsch, 2009), node2vec (node2vec) (Grover & Leskovec, 2016), DeepWalk (DeepWalk) (Perozzi et al., 2014), and LINE (LINE) (Tang et al., 2015). For all methods, we set the number of embedding dimensions to 128. For LINE, node2vec, and DeepWalk, we set the number of walkers to 40 and the number of the walk length to 80 following Ref. (Kojaku et al., 2024). We used the default hyperparameters used in the original papers unless otherwise specified.

#### A.2.3. GRAPH NEURAL NETWORKS

Graph neural networks (GNNs) learn the vector representation,  $\vec{u}_i$ , for each node  $i$  of the network by using neural networks. The prediction score  $s_{ij}$  is given by the dot product  $\vec{u}_i^\top \vec{u}_j$  between any two node vectors. We also explore several graph neural network (GNN) architectures for link prediction, leveraging the PyTorch Geometric library (Fey & Lenssen, 2019). The GNN methods we employ include: Graph Convolutional Network (GCN) (Kipf & Welling, 2017), Graph SAGE (GraphSAGE) (Hamilton et al., 2017), Graph Attention Network (GAT) (Veličković et al., 2018), and Graph Isomorphism Network (GIN) (Xu et al., 2019). We used held-out validation to tune the number of hidden layers (1 or 2) and the number of dimensions in each hidden layer (64, 128, or 256) with the validation set consisting of 10% of the edges. We use ReLu activation and a dropout rate of 0.2. The node features are the 64 principal eigenvectors of the adjacency matrix, and we extend the feature vector by adding a 64-dimensional vector with each element being generated from an independent Gaussian distribution with mean 0 and standard deviation 1 by following Ref. (Sato et al., 2021; Abboud et al., 2020). We train GNNs on the link prediction task for 250 epochs with a dropout rate of 0.2, using the Adam optimizer at a learning rate of 0.01. We use the ‘LinkNeighborLoader’ from PyTorch Geometric to generate training mini-batches. This loader samples both positive and negative edges, along with 30 immediate neighbors and 10 secondary neighbors sampled by random walks for each node involved in these edges (Hamilton et al., 2017). The batch size is set to 5000.

We also tested BUDDY GNN, which achieves a competitive performance on the link prediction task (Chamberlain et al., 2023). We employed hyperparameter tuning for the number of hidden channels (256 or 1024), and the feature dropout rate (0.05 or 0.2) with the validation set consisting of 10% of the edges. We set the number of hops to 2 because it consistently achieved a better performance. For other hyperparameters, we used the default values used in the original implementation.

#### A.2.4. NEWORK MODELS

We use two stochastic block models (SBM) (Fortunato, 2010; Fortunato & Hric, 2016; Fortunato & Newman, 2022; Peixoto, 2013) and the degree-corrected SBM (Karrer & Newman, 2011; Peixoto, 2013; Gra). These models estimate the probability  $P(i, j)$  that an edge exists between two nodes, which serves as the prediction score  $s_{ij}$ . We fit the SBMs using the graph tool package (Gra). We select the number of blocks that minimize the description length and use default settings for other parameters.

### A.3. Pseudo-code for the degree-corrected link prediction benchmark

The pseudo-code for the degree-corrected link prediction benchmark is shown in Table. 1.

---

#### Algorithm 1 Degree-corrected link prediction benchmark

```

Input: Graph  $G(\mathcal{V}, \mathcal{E})$ , Sampling fraction  $\beta \in [0, 1]$  for positive edges
Output: Set of negative edges  $\mathcal{E}_{\text{neg}}$  and set of positive edges  $\mathcal{E}_{\text{pos}}$ 
Generate  $\mathcal{E}_{\text{pos}}$  by randomly sampling a  $\beta$  fraction of edges in  $\mathcal{E}$ 
Initialize  $\mathcal{E}_{\text{neg}} \leftarrow \emptyset$ 
Create a node list  $L$  where each node  $i \in \mathcal{V}$  with degree  $k_i$  appears  $k_i$  times
while  $|\mathcal{E}_{\text{neg}}| < |\mathcal{E}_{\text{pos}}|$  do
    Randomly select two nodes  $i, j$  from  $L$  with replacement
    if  $(i, j) \notin \mathcal{E}$  and  $(i, j) \notin \mathcal{E}_{\text{neg}}$  and  $i \neq j$  then
         $\mathcal{E}_{\text{neg}} \leftarrow \mathcal{E}_{\text{neg}} \cup \{(i, j)\}$ 
    end if
end while
return  $\mathcal{E}_{\text{neg}}, \mathcal{E}_{\text{pos}}$ 

```

---

Table 1. Link prediction algorithms. “pyg” refers to PyTorch Geometric.

	Algorithm	Reference	Code	Notation
Topology based	Preferential attachment	(Barabási & Pósfai, 2016)	ourselves	PA
	Common neighbors	(Liben-Nowell & Kleinberg, 2003)	ourselves	CN
	AdamicAdar	(Adamic & Adar, 2003)	ourselves	AA
	Jaccard index	(Liben-Nowell & Kleinberg, 2003)	ourselves	JI
	Resource allocation	(Zhou et al., 2007; 2009)	ourselves	RA
	Local Random Walk	(Liu & Lü, 2010)	ourselves	LRW
	Local Path Index	(Lü et al., 2009)	ourselves	LPI
	MLP-deg		ourselves	MLP-deg
	MLP-topo		ourselves	MLP-topo
	Linear model		ourselves	Linear
Graph embedding	Laplacian EigenMap	(Belkin & Niyogi, 2003)	ourselves	EigenMap
	Spectral modularity	(Nadakuditi & Newman, 2012)	ourselves	Mod
	Non-backtracking embedding	(Krzakala et al., 2013)	ourselves	NB
	FastRP	(Chen et al., 2019)	ourselves	FastRP
	Adjacency matrix w/ the exponential kernel	(Kondor & Lafferty, 2002), (Kunegis & Lommatsch, 2009)	ourselves	Exp-A
	Laplacian w/ the exponential kernel	(Kondor & Lafferty, 2002), (Kunegis & Lommatsch, 2009)	ourselves	Exp-L
	Normalized Laplacian w/ the exponential kernel	(Kondor & Lafferty, 2002), (Kunegis & Lommatsch, 2009)	ourselves	Exp-NL
	Adjacency matrix w/ the von Neumann kernel	(Kondor & Lafferty, 2002), (Kunegis & Lommatsch, 2009)	ourselves	vN-A
	Laplacian w/ the von Neumann kernel	(Ito et al., 2005), (Kunegis & Lommatsch, 2009)	ourselves	vN-L
	Normalized Laplacian w/ the von Neumann kernel w/ the von Neumann kernel	(Ito et al., 2005), (Kunegis & Lommatsch, 2009)	ourselves	vN-NL
	LINE	(Tang et al., 2015)	gensim (Rehurek & Sojka, 2011), (Abraham, 2020)	LINE
	DeepWalk	(Perozzi et al., 2014)	gensim (Rehurek & Sojka, 2011), (Abraham, 2020)	DeepWalk
	node2vec	(Grover & Leskovec, 2016)	gensim (Rehurek & Sojka, 2011), (Abraham, 2020)	node2vec
			gensim (Chamberlain et al., 2023)	BUDDY
Graph neural networks	Graph Convolutional Network	(Kipf & Welling, 2017)	pyg (Fey & Lenssen, 2019)	GCN
	Graph SAGE	(Hamilton et al., 2017)	pyg (Fey & Lenssen, 2019)	GraphSAGE
	Graph Attention Network	(Veličković et al., 2018)	pyg (Fey & Lenssen, 2019)	GAT
	GIN	(Xu et al., 2019)	pyg (Fey & Lenssen, 2019)	GIN
Network model	BUDDY GNN	(Chamberlain et al., 2023)	(Chamberlain et al., 2023)	BUDDY
	Stochastic block model	(Fortunato, 2010; Fortunato & Hric, 2016), (Fortunato & Newman, 2022; Peixoto, 2013)	graph tool (Gra)	SBM
	Degree-corrected stochastic block model	(Karrer & Newman, 2011; Peixoto, 2013; Gra)	graph tool (Gra)	dcSBM

#### A.4. Additional analysis methods

We use the following additional analysis methods in this paper. We fit a log-normal distribution to the degree distribution of the graphs by using the moment method implemented in the `scipy.stats.lognorm` package (Virtanen et al., 2020). We fit a powerlaw distribution to the degree distribution of the graphs by using the maximum likelihood method implemented in the `powerlaw` package (Alstott et al., 2014). We compute the RBO score by using the `rbo` package (`rbo`).

### B. AUC-ROC for the preferential attachment method

Let us first derive the degree distribution of nodes in the positive edges. By substituting Eq. 3 into Eq. 1 in the main text, we derive the degree distribution of nodes in the positive edges as:

$$\begin{aligned} p_{\text{pos}}(k) &= \frac{k}{\langle k \rangle} \frac{1}{\sqrt{2\pi}\sigma k} \cdot \exp \left[ -\frac{(\ln k - \mu)^2}{2\sigma^2} \right] \\ &= \frac{1}{\sqrt{2\pi}\sigma k} \exp \left[ -\frac{1}{2\sigma^2} ((\ln k)^2 - 2\mu \ln k + \mu^2) + \ln k - \mu - \sigma^2/2 \right] \\ &= \frac{1}{\sqrt{2\pi}\sigma k} \exp \left[ -\frac{1}{2\sigma^2} ((\ln k)^2 - 2(\mu + \sigma^2) \ln k + \mu^2 + 2\mu\sigma^2 + \sigma^4) \right] \\ &= \frac{1}{\sqrt{2\pi}\sigma k} \exp \left[ -\frac{(\ln k - \mu - \sigma^2)^2}{2\sigma^2} \right] \end{aligned} \quad (4)$$

This is the probability density function of a log-normal distribution with mean  $\mu + \sigma^2$  and variance  $\sigma^2$ , i.e.,

$$p_{\text{pos}}(k) = \text{LogNorm}(k | \mu + \sigma^2, \sigma^2). \quad (5)$$

Equation 5 indicates that the degree distribution for nodes in the positive edges also follows a log-normal distribution, parameterized by  $\mu + \sigma^2$  and  $\sigma$ .

We derive the AUC-ROC for PA by leveraging a unique characteristic of log-normal distributions, i.e., the logarithm  $\ln k$  of log-normally-distributed degree  $k$  follows a normal distribution with mean  $\mu$  and variance  $\sigma^2$ , i.e.,

$$P(\ln k) = \text{Norm}(k | \mu, \sigma^2), \text{ where } \text{Norm}(k | \mu, \sigma^2) = \frac{1}{\sqrt{2\pi}\sigma} \exp \left[ -\frac{(k - \mu)^2}{2\sigma^2} \right]. \quad (6)$$

We assume no degree assortativity in the graph, where  $P(k_i^+, k_j^+) = P(k_i)P(k_j)$ . Although empirical graphs often exhibit degree assortativity, our results indicate that it does not significantly impact the AUC-ROC (Appendix E.2). For the negative edges, the distribution for  $\ln s_{i-,j-} = \ln k_i^- + \ln k_j^-$  follows a normal distribution with mean  $2\mu$  and variance  $2\sigma^2$ , as the sum of independent normal variables also forms a normal distribution with additive means and variances (Bishop, 2006), i.e.,

$$P(\ln s_{i-,j-}) = \text{Norm}(\ln s_{i-,j-} | 2\mu, 2\sigma^2). \quad (7)$$

For the positive edges, the degree distribution also follows a log-normal distribution (Eq. 5). Thus, the distribution for  $\ln s_{i+,j+} = \ln k_i^+ + \ln k_j^+$  is given by

$$P(\ln s_{i+,j+}) = \text{Norm}(\ln s_{i+,j+} | 2\mu + 2\sigma^2, 2\sigma^2). \quad (8)$$

Thus, we have

$$\begin{aligned} \text{AUC-ROC} &= P(\ln s^- < \ln s^+) \\ &= \int_{-\infty}^{\infty} \text{Norm}(x^- | 2\mu, 2\sigma^2) \left[ 1 - \int_{-\infty}^{x^-} \text{Norm}(x^+ | 2\mu + 2\sigma^2, 2\sigma^2) dx^+ \right] dx^- \\ &= 1 - \int_{-\infty}^{\infty} \text{Norm}(x^- | 2\mu, 2\sigma^2) \int_{-\infty}^{x^-} \text{Norm}(x^+ | 2\mu + 2\sigma^2, 2\sigma^2) dx^+ dx^- \end{aligned} \quad (9)$$

We reparameterize Eq. 9 by using  $z^\pm = \frac{x^\pm - 2\mu}{\sqrt{2}\sigma}$ . Noting that  $\text{Norm}(x^- | 2\mu, 2\sigma^2) \cdot \sqrt{2}\sigma = \text{Norm}(z^- | 0, 1)$  and  $dx^\pm = (\sqrt{2}\sigma)dz^\pm$ , we have

$$\begin{aligned} P(\ln s^- < \ln s^+) &= 1 - \int_{-\infty}^{\infty} \text{Norm}(x^- | 2\mu, 2\sigma^2) \int_{-\infty}^{x^-} \text{Norm}(x^+ | 2\mu + 2\sigma^2, 2\sigma^2) \cdot dx^+ dx^- \\ &= 1 - \int_{-\infty}^{\infty} \text{Norm}(z^- | 0, 1) \int_{-\infty}^{z^-} \text{Norm}(z^+ - \sqrt{2}\sigma | 0, 1) dz^+ dz^- \\ &= 1 - \int_{-\infty}^{\infty} \text{Norm}(z^- | 0, 1) \Phi(z^- - \sqrt{2}\sigma) dz^-, \end{aligned} \quad (10)$$

where  $\Phi(z^-)$  is the cumulative distribution function for the standard normal distribution, i.e.,  $\Phi(z^-) = \int_{-\infty}^{z^-} \text{Norm}(y | 0, 1) dy$ . We recognize that

$$\int_{-\infty}^{\infty} \text{Norm}(z^- | 0, 1) \Phi(z^- - \sqrt{2}\sigma) dz^- = \mathbb{E}_{z^-} [\Phi(z^- - \sqrt{2}\sigma)]. \quad (11)$$

Here,  $\mathbb{E}_{z^-}$  denotes the expectation over normally distributed random variable  $z^-$ . The cumulative distribution function  $\Phi$  can be expressed using another normally distributed random variable  $y$  as:

$$\Phi(z^- - \sqrt{2}\sigma) = P(y < z^- - \sqrt{2}\sigma | z^-) = P(y - z^- > \sqrt{2}\sigma | z^-). \quad (12)$$

Applying the law of total probability ( $P(A) = \mathbb{E}_X [P(A | X)]$ ), we have:

$$\mathbb{E}_{z^-} [\Phi(z^- - \sqrt{2}\sigma)] = \mathbb{E}_{z^-} [P(y - z^- > \sqrt{2}\sigma | z^-)] = P(y - z^- > \sqrt{2}\sigma). \quad (13)$$

Since  $y$  and  $z^-$  are both normally distributed, their difference  $y - z^-$  is normally distributed with mean 0 and variance 2. Thus,

$$P(y - z^- > \sqrt{2}\sigma) = 1 - \Phi\left(\frac{\sqrt{2}\sigma}{\sqrt{2}}\right) = 1 - \Phi(\sigma) \quad (14)$$

Substituting this into Eq. 10, we have:

$$P(s^- < s^+) = \Phi(\sigma). \quad (15)$$

## C. AUC-ROC for asymmetric degree-proportional sampling

We analyze the behavior of AUC-ROC for PA when link prediction is evaluated using an asymmetric negative sampling scheme. In this set up, a method is evaluated by a set of triplets  $(i, j^+, j^-)$  where  $(i, j^+)$  is sampled from the observed edges, and  $j^-$  is sampled uniformly at random over nodes. This setup is used in Bayesian Personalized Ranking (BPR), where training triples are drawn uniformly from the observed interaction set (Rendle et al., 2009). We focus on the performance of PA under this sampling scheme and prove that, as the degree distribution becomes increasingly skewed, the AUC-ROC of PA approaches 1, as is the case of the uniform sampling of negative edges.

Let us first recall that the degree of node  $j^-$  in the negative edges follows the original degree distribution  $p(k)$  because node  $j^-$  is selected uniformly at random from all nodes. Conversely, nodes  $i$  and  $j^+$  have degrees following  $p_{\text{pos}}(k)$  (Eq. 1) due to the friendship paradox (Section 2.3). Specifically, a node with degree  $k$  appears  $k$  times among observed edges, and as a result, its degree distribution is proportional to  $kp(k)$ , and hence aligns with  $p_{\text{pos}}(k)$ .

We are interested in the AUC-ROC of PA for the positive and negative edges as  $(i^+, j^+)$  and  $(i^-, j^-)$ , i.e.,

$$P(s^- < s^+) = P(\log k_{i^-} + \log k_{j^-} < \log k_{i^+} + \log k_{j^+}). \quad (16)$$

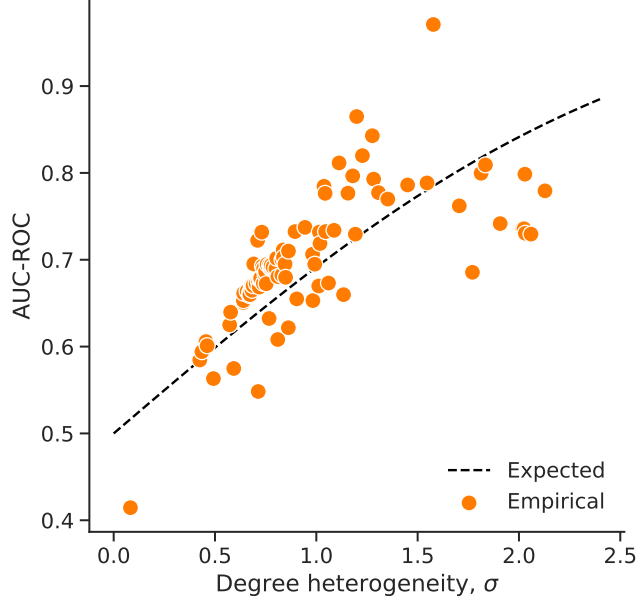


Figure 4. AUC-ROC for PA under the asymmetric negative sampling.

Assuming that  $p(k)$  is a log-normal distribution, the sum  $\log k_{i-} + \log k_{j-}$  involves two normally distributed random variables,  $\log k_{i-}$  and  $\log k_{j-}$ , with means  $\mu$  and  $\mu + \sigma^2$ , respectively, and each with variance  $\sigma^2$ . Consequently, their sum is also normally distributed with mean  $2\mu + \sigma^2$  and variance  $2\sigma^2$ . Denoting by  $x^\pm = \log k_{i\pm} + \log k_{j\pm}$ , we have:

$$\begin{aligned} P(s^- < s^+) &= \int_{-\infty}^{\infty} \text{Norm}(x^- | 2\mu + \sigma^2, 2\sigma^2) \left[ 1 - \int_{-\infty}^{x^-} \text{Norm}(x^+ | 2\mu + 2\sigma^2, 2\sigma^2) dx^+ \right] dx^- \\ &= 1 - \int_{-\infty}^{\infty} \text{Norm}(x^- | 2\mu + \sigma^2, 2\sigma^2) \int_{-\infty}^{x^-} \text{Norm}(x^+ | 2\mu + 2\sigma^2, 2\sigma^2) dx^+ dx^- \end{aligned}$$

By reparameterizing  $x^\pm$  by using  $z^\pm = \frac{x^\pm - (2\mu + \sigma^2)}{\sqrt{2}\sigma}$ , we have

$$\begin{aligned} P(s^- < s^+) &= 1 - \int_{-\infty}^{\infty} \text{Norm}(z^- | 0, 1) \int_{-\infty}^{z^-} \text{Norm}\left(z^+ - \frac{\sigma}{\sqrt{2}} | 0, 1\right) dz^+ dz^- \\ &= 1 - \int_{-\infty}^{\infty} \text{Norm}(z^- | 0, 1) \Phi\left(z^- - \frac{\sigma}{\sqrt{2}}\right) dz^- \end{aligned} \quad (17)$$

By taking the same derivation steps as in Eqs. 11–15, we have:

$$P(s^- < s^+) = \Phi\left(\frac{\sigma}{2}\right). \quad (18)$$

Since  $\Phi$  is a monotonically increasing function, the AUC-ROC is also an increasing function of  $\sigma$ . The rate of increase is less than the AUC-ROC for the uniform sampling of negative edges (Eq. 15). This can be understood by noting that one endpoint node  $i$  of the negative edges in the asymmetric sampling is sampled from the observed edges, which is more likely to have a higher degree than that of the negative edges sampled uniformly at random.

Empirical validation of Eq. 18 confirmed that the AUC-ROC for PA under the asymmetric negative sampling closely follows that for empirically measured AUC-ROC (Fig. 4).

## D. Decomposition analysis of AUC-ROC scores

A key concern with the standard benchmark is that link prediction methods may overfit to nodes with high degrees. To investigate this systematically, we developed a decomposition analysis of the AUC-ROC scores that reveals how different

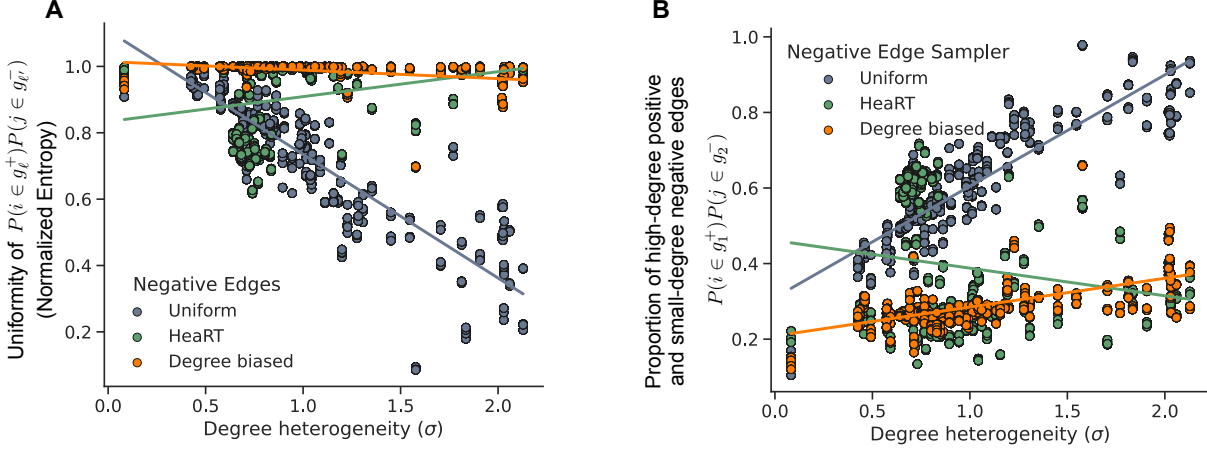


**Figure 5.** Decomposition of the AUC-ROC score by degree combinations. Each dot represents a graph. **A:** Uniformity of  $P(i \in g_\ell^+)P(j \in g_\ell^-)$  quantified by the normalized entropy,  $H$ . **B:** Probability  $P(i \in g_1^+)P(j \in g_2^-)$  that the positive edges are sampled from the high-degree node group  $g_1^+$  and the negative edges are sampled from the low-degree node group  $g_2^-$ .

groups of nodes contribute to the overall performance metrics.

The AUC-ROC score—the probability that a positive sample has a higher score than a negative sample—can be decomposed into conditional scores by partitioning the evaluation edges into groups. Specifically, if we partition edges into groups  $g_1$  and  $g_2$ , the AUC-ROC score can be written as:

$$P(s^+ > s^-) = \sum_{\ell=1}^2 \sum_{\ell'=1}^2 P(s_i^+ > s_j^- | i \in g_\ell^+, j \in g_{\ell'}^-) P(i \in g_\ell^+) P(j \in g_{\ell'}^-) \quad (19)$$

where  $s_i^+$  and  $s_j^-$  are the scores of the positive and negative edges given by a link prediction method, respectively, and  $g_\ell^+$  and  $g_\ell^-$  are the positive and negative edges in the  $\ell$ -th group, respectively. Probability  $P(s_i^+ > s_j^- | i \in g_\ell^+, j \in g_{\ell'}^-)$  represents the conditional AUC-ROC score for a positive edge sampled from  $g_\ell^+$  and a negative edge sampled from  $g_{\ell'}^-$ . Probability  $P(i \in g_\ell^+)P(j \in g_{\ell'}^-)$  represents the probability that a positive edge is sampled from  $g_\ell^+$  and a negative edge is sampled from  $g_{\ell'}^-$ . We note that  $P(i \in g_\ell^+)P(j \in g_{\ell'}^-)$  is determined by the sampling of positive and negative edges and independent of the link prediction methods.

Based on this decomposition, we investigate the impact of edges of different node degrees on the overall AUC-ROC scores. Specifically, we partition edges into two equal-sized groups based on the degree product  $z = k_i k_j$  of their endpoint nodes, with  $g_1$  having  $z \geq \text{median}$  and  $g_2$  having  $z < \text{median}$ . We tested multiple definitions of  $z$  including degree sum ( $k_i + k_j$ ), minimum degree ( $\min(k_i, k_j)$ ), and maximum degree ( $\max(k_i, k_j)$ ), finding consistent results across all definitions.

To measure how uniformly different groups contribute to the AUC-ROC score, we use normalized entropy:

$$H = - \sum_{\ell=1}^2 \sum_{\ell'=1}^2 P(i \in g_\ell^+)P(j \in g_{\ell'}^-) \log P(i \in g_\ell^+)P(j \in g_{\ell'}^-) / \log 4 \quad (20)$$

The entropy is bounded between 0 and 1, where 0 indicates that the AUC-ROC score is determined by a single group pair and 1 indicates that the AUC-ROC score is evenly distributed across all group pairs.

We observe that the standard benchmark exhibits notable disparity compared to HeaRT and degree-corrected benchmark, indicating that the contribution to the AUC-ROC score in the standard benchmark can be heavily skewed toward certain combinations of node degrees (Fig. 5A). This disparity becomes even more pronounced in networks with high degree heterogeneity ( $H < 0.5$  and  $\sigma > 1.5$ ). This disparity is caused by a single group pair—positive edges from high-degree

*Table 2.* Mean absolute coefficients from logistic regression analysis across different graphs. Features were orthogonalized to eliminate collinearity, and coefficients were normalized by the feature L2 norm. Larger coefficients indicate greater importance in link prediction.

Topological Feature	Mean Absolute Coefficient		
	All Graphs	Graphs with $\sigma > 1$	Graphs with $\sigma > 1.5$
Random walk	11.52	10.68	9.01
Degree product	8.79	17.19	28.00
Resource allocation	2.81	4.53	6.88
Adamic-Adar	1.35	2.35	2.89
Jaccard index	0.89	1.06	0.17

nodes and negative edges from low-degree nodes—with  $P(i \in g_1^+)P(j \in g_2^-) > 0.7$  for  $\sigma > 1.5$  (Fig. 5B). This means that for highly heterogeneous networks, more than 70% of the AUC-ROC score is determined by cases that can be easily classified using degree alone. The degree-corrected benchmark achieves high uniformity ( $H \approx 1$ ) across group pairs (Fig. 5A), indicating that the contribution to the AUC-ROC score is approximately evenly distributed across different degree groups.

To validate these findings further, we performed additional experiments using logistic regression to analyze the importance of features. The model was trained with resource allocation, Jaccard index, Adamic Adar, local random walk, and degree product. To ensure a fair comparison, we orthogonalized the non-degree features with respect to the degree to eliminate collinearity effects. Additionally, we use ridge regularization to further mitigate the effect of collinearity. We use the scikit-learn package (Pedregosa et al., 2011) to perform the logistic regression with the default ridge regularization strength. To make the regression coefficients comparable, we normalize the features by their L2 norm before training the model. The results showed that in networks with high degree heterogeneity ( $\sigma > 1$ ), the degree product emerges as significantly important, with its coefficient 1.7 3 times as large as the second most important feature (Table. 2).

This dominance of degree-based prediction is particularly concerning because it indicates that learning-based methods can achieve high benchmark performance by primarily exploiting degree information rather than learning more complex structural patterns. This “shortcut” is precisely what our degree-corrected benchmark aims to prevent.

These results provide strong quantitative support for our argument that the standard benchmark’s evaluation is dominated by easily classified degree-based cases, potentially leading to suboptimal model training. The degree-corrected benchmark successfully addresses this issue by ensuring more uniform contributions from different degree groups, leading to a more meaningful evaluation of link prediction methods.

## E. Robustness analysis

### E.1. Method ranking by HeaRT benchmark

The ranking of methods by the HeaRT benchmark is shown in Fig. 6. The results show that PA achieves the highest AUC-ROC scores among all methods in the HeaRT benchmark, contrasting sharply with its lowest performance in the degree-corrected benchmark. This indicates that degree bias may not be reduced by HeaRT, which reduces the distance-based bias.

### E.2. Impact of degree assortativity on the AUC-ROC for PA

We have assumed that the graph has no degree assortativity, meaning that  $P(k_i, k_j) = P(k_i)P(k_j)$ . Although this assumption may not always hold, it provides a good approximation for the AUC-ROC behavior for PA. Although the assortativity varies across graphs, the AUC-ROC for PA still closely follows Eq. (9) in the main text (Fig. 7).

### E.3. AUC-ROC for PA for scale-free networks

We have assumed that the graph exhibits the heterogeneous degree distributions characterized by the log-normal distribution. An alternative model of the degree distribution is the powerlaw distribution (Barabási & Bonabeau, 2003). Here, we show that our results also hold for the powerlaw degree distribution, i.e., the AUC-ROC for PA increases as the degree

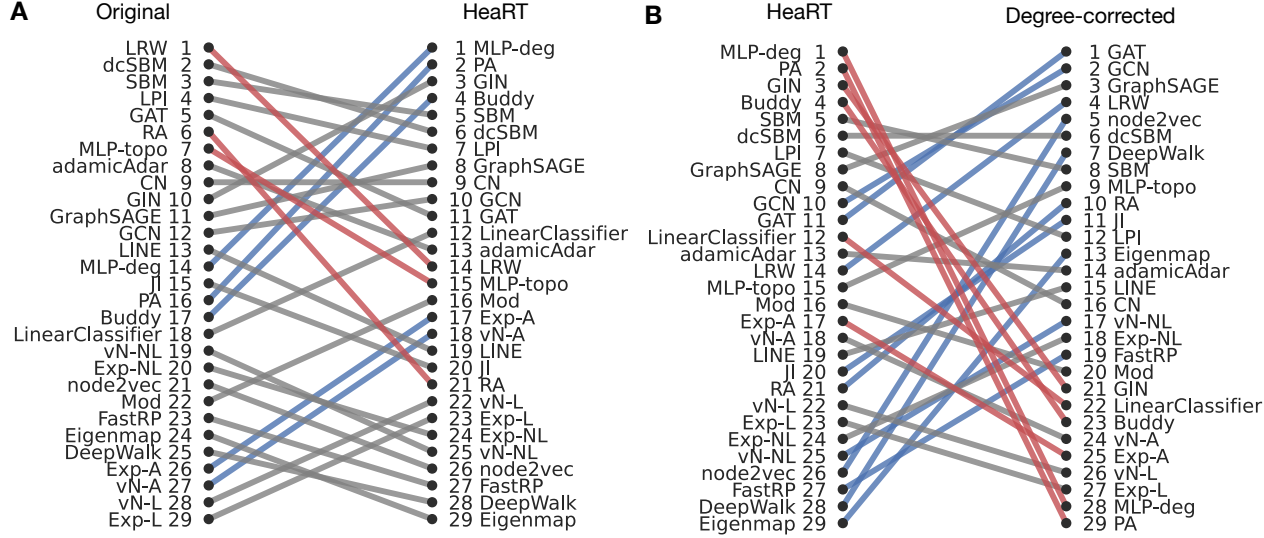


Figure 6. Comparison of the AUC-ROC scores between the original, degree-corrected, and the HeaRT benchmarks.

heterogeneity increases.

We compute the AUC-ROC for PA for graphs with powerlaw degree distribution. Computing AUC-ROC  $P(k_{i-}k_{j-} \leq k_{i+}k_{j+})$  is not trivial because it involves multiplicative convolution of two probability distributions, which are hard to compute for the power law degree distribution. To circumvent this problem, we consider the lower-bound by focusing on  $k_{i-} \leq k_{i+}$  and  $k_{j-} \leq k_{j+}$ , which is the subset of all combinations of  $(k_{i-}, k_{i+}, k_{j-}, k_{j+})$  leading to  $k_{i-}k_{j-} \leq k_{i+}k_{j+}$ , i.e.,

$$P(k_{i-} < k_{i+}) \cdot P(k_{j-} < k_{j+} | k_{i-}, k_{i+}) \leq P(k_{i-}k_{j-} < k_{i+}k_{j+}) \quad (21)$$

Assuming that the graph has no degree assortativity (i.e.,  $P(k_i, k_j) = P(k_i)P(k_j)$ ), we obtain the lower bound for the AUC-ROC:

$$P(k_{i-} < k_{i+}) \geq P(k_{i-} < k_{i+})^2 = \left[ \sum_{k=1}^{\infty} p_{\text{neg}}(k) \sum_{\ell=k}^{\infty} p_{\text{pos}}(\ell) \right]^2. \quad (22)$$

Now, let us compute the lower bound by assuming that the degree distribution follows a power-law (Clauset et al., 2009):

$$p(k) = \frac{1}{\zeta(\alpha, k_{\min})} k^{-\alpha}, \quad (k \geq k_{\min}), \quad \text{where } \zeta(\alpha, k_{\min}) = \sum_{\ell=k_{\min}}^{\infty} \ell^{-\alpha}, \quad (23)$$

where  $\zeta$  is the Hurwitz zeta function, and  $k_{\min}$  is the minimum degree. By substituting Eq. (1) in the main text into Eq. 23, we have  $p_{\text{pos}} = k^{-\alpha+1}/\zeta(\alpha-1, k_{\min})$ . By noting that  $\sum_{\ell=k}^{\infty} p(\ell) = \zeta(\alpha, k)/\zeta(\alpha, k_{\min})$  (Clauset et al., 2009), we have

$$P(k_{i-} < k_{i+})^2 = \left[ \frac{1}{\zeta(\alpha, k_{\min})\zeta(\alpha-1, k_{\min})} \sum_{k=k_{\min}}^{\infty} k^{-\alpha}\zeta(\alpha-1, k) \right]^2. \quad (24)$$

Numerical calculation shows that the lower bound  $P(k_{i-} < k_{i+})^2$  approaches 1 as  $\alpha \rightarrow 2$  (Fig. 7). Additional validation using the Price network with  $N = 10^4$  nodes and  $M = 10^5$  edges, where  $p(k) \propto k^{-\alpha}$ , confirms that PA achieves higher AUC-ROC than the lower-bound and reaches near-maximal AUC-ROC scores for  $\alpha \approx 2$ .

We can also compute the AUC score using the Mann-Whitney U statistic (Fig. 8). Let us take a graph  $G$  with the set of nodes given by  $\mathcal{V}$ . We sample nodes  $i, j$  with degrees  $k_i^+, k_j^+$  forming the positive set of edges from  $p_{\text{pos}}$ , and nodes  $m, n$  with

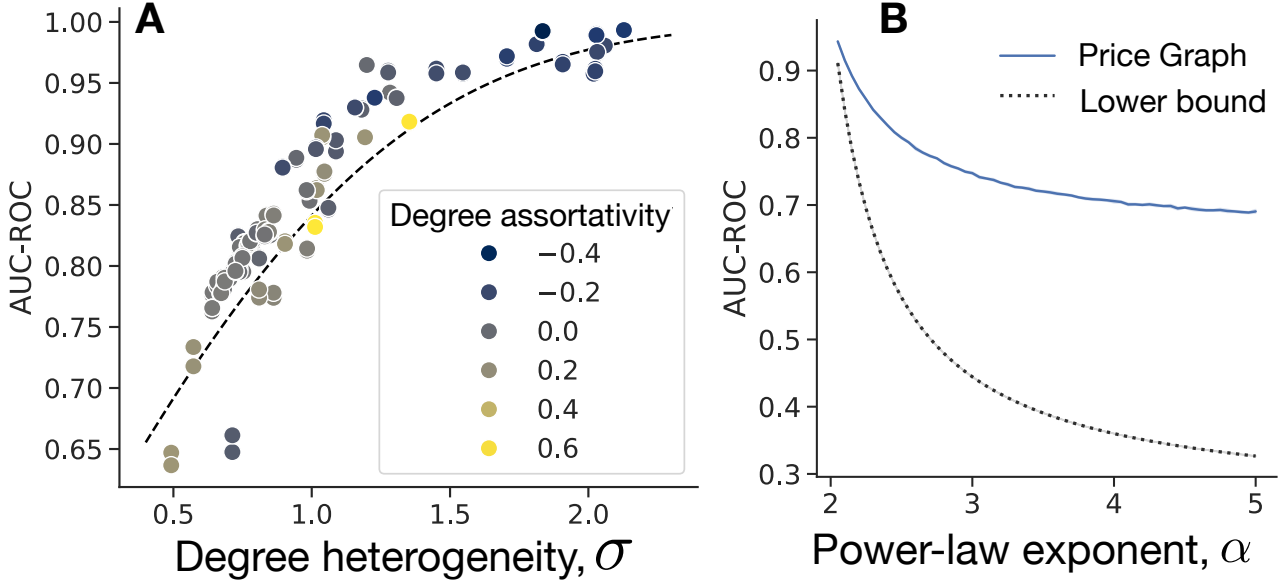


**Figure 7.** The AUC-ROC for PA as a function of degree heterogeneity. **A:** The AUC-ROC for the empirical graphs and that expected by node degree (Eq. (9) in the main text). The colors represent the degree assortativity. **B:** Lower bound for the AUC-ROC for the powerlaw degree distributions. The dashed line represents the lower bound for the AUC-ROC for the powerlaw distribution. The blue line represents the AUC-ROC for PA for the Price graph with  $N = 10^4$  nodes and  $M = 10^5$  edges.

degrees  $k_m^-, k_n^-$  forming the negative set of edges from  $p_{neg}$ . Then  $P(k_i^+ k_j^+ > k_m^-, k_n^-) \forall i, j, k, m \in \mathcal{V}$  is the AUC score and is given by  $\frac{U}{n_1 n_2}$  where U is the Mann-Whitney U statistic and  $n_1, n_2$  are sizes of the positive and negative edge sets respectively (Mason & Graham, 2002). We sample the random variables  $k_i^+, k_j^+$  using the ‘Power\_Law’ function from the powerlaw package (Alstott et al., 2014) with degree exponent  $\alpha - 1$  since  $p_{pos}(k) \sim k^{-(\alpha-1)}$ . Similarly, we sample  $k_m^-, k_n^-$  with degree exponent  $\alpha$  since  $p_{neg}(k) \sim k^{-\alpha}$ . Fig. 8 aligns with our findings in Fig. 7B, i.e., PA reaches near maximal AUC-ROC scores as  $\alpha \rightarrow 2$ .

#### E.4. Analysis of large-scale networks

To test whether the degree bias persists in large-scale real-world networks, we analyzed two large-scale citation networks, i.e., the Science of Science (SciSci) citation network (Lin et al., 2023), which represents citations between more than 95M publications across all sciences, and the USPTO citation network (Patent & Office, 2023), consisting of more than 7M patents in the US.

We followed the same procedure as our main analysis to test for degree bias, measuring the AUC-ROC score of the preferential attachment model. The results strongly supported our theoretical predictions: PA achieved an AUC-ROC score of 0.9452 for SciSci and 0.881 for USPTO, closely matching our theoretical predictions of 0.9479 and 0.918, respectively. With the degree-corrected benchmark, the AUC-ROC scores for PA decrease for both graphs, e.g., 0.5018 for SciSci and 0.4818 for the USPTO.

While we do not run other link prediction methods on these networks due to computational constraints, these results provide strong evidence that our findings about degree bias are not limited to smaller networks but represent a fundamental characteristic of the standard link prediction benchmark.

#### E.5. Parameter sensitivity in the analysis of performance alignment with the recommendation task

Normalized Discounted Cumulative Gain (NDCG) is a widely used metric in information retrieval and recommendation systems that evaluates the quality of ranked lists by considering both the relevance of items and their positions in the ranking. Unlike metrics such as precision or recall that treat all positions equally, NDCG applies a logarithmic discount factor that

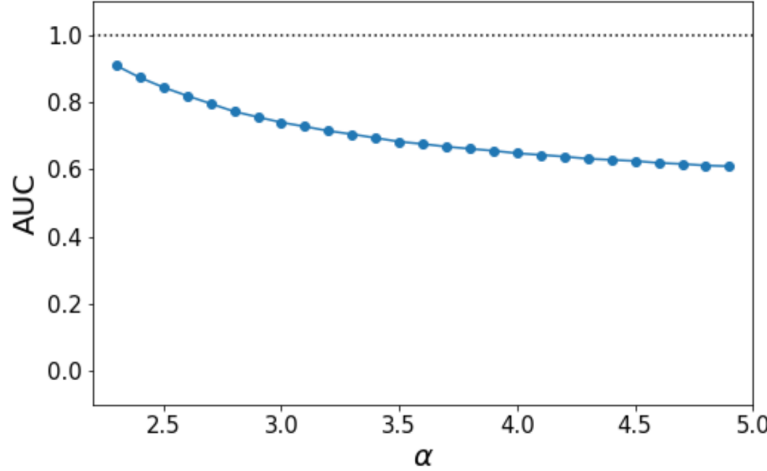


**Figure 8.** The influence of degree heterogeneity on the performance of the preferential attachment (PA) link prediction model in graphs with a power law degree distribution. The degree heterogeneity is governed by the power law exponent  $\alpha$ . As  $\alpha$  increases, the heterogeneity decreases. PA reaches near maximal AUC-ROC scores (1) as  $\alpha \rightarrow 2$ . For each  $\alpha$ , we generate 20 batches, each with 5000 samples of  $k_i^+, k_j^+, k_m^-, k_n^-$ . The dots indicate the average AUC score obtained via the Mann-Whitney U statistic. Standard mean errors are smaller than the dots.

penalizes relevant items appearing lower in the ranking, reflecting the diminishing probability that users will examine items further down a list. Formally, for a ranked list of items, NDCG@K is computed by first calculating the Discounted Cumulative Gain (DCG) up to position K:

$$\text{NDCG@K for node } i = \sum_{j=1}^K \frac{Y_{ij}}{\log_2(i+1)}, \quad (25)$$

where  $Y_{ij}$  is the indicator function of node  $j$  is connected with  $i$  in the test data ( $Y_{ij} = 1$ ), and otherwise  $Y_{ij} = 0$ . This value is then normalized by dividing by the DCG of the ideal ranking (IDCG), where all relevant items are placed at the top positions:

$$\text{NDCG@K} = \frac{\text{DCG@K}}{\text{IDCG@K}}. \quad (26)$$

In our link prediction evaluation, we use NDCG@100 to assess how well different methods rank true connections among their top 100 predictions.

We compute the similarity of two rankings with rank-biased overlap (RBO) (Webber et al., 2010). RBO assesses the similarity of two rankings by examining the overlap of top-performing methods. Define  $U_{k,1}$  as the set of methods ranked in the top  $k$  positions in ranking 1, and  $U_{k,2}$  similarly for ranking 2. Then, RBO computes a weighted average of the similarity of the top  $k$  methods by

$$\text{RBO}(S, T, p) := (1 - p) \sum_{k=1}^{\infty} p^{k-1} \frac{|U_{k,1} \cap U_{k,2}|}{k}, \quad (27)$$

where  $p$  controls the importance of the top performer, with a smaller  $p$  value placing more weight on the top performer. We use  $p = 0.5$  for the results in the main text. We find consistent results across different  $p$  values (Fig. 9A and B). Additionally, we find consistent results for a different number of recommendations  $K$  (Fig. 9C and D).

We also compute the vertex-centric max precision recall at  $K$  (VCMPR@K) metric (Menand & Seshadhri, 2024) to evaluate the performance of the link prediction methods. This metric is proposed for evaluating link prediction methods in

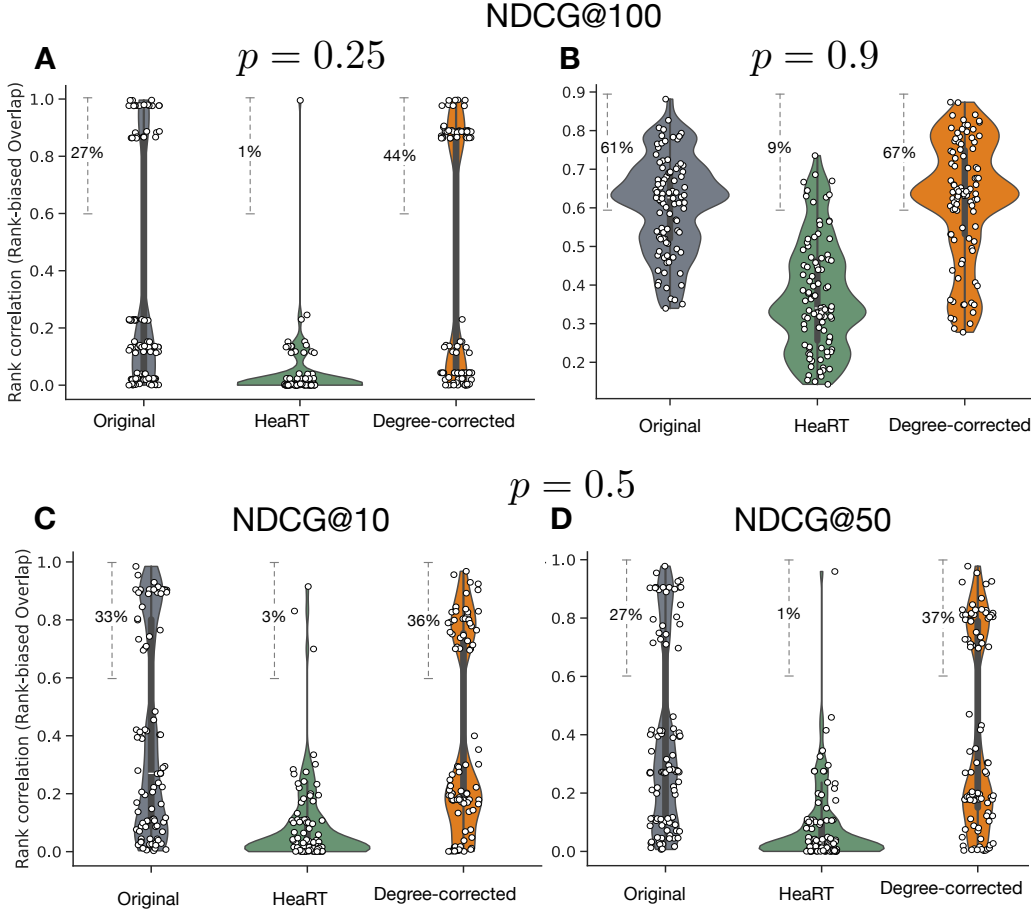


Figure 9. RBO for different  $p$  values and different numbers  $K$  of recommendations.

recommendation settings. The VCMPR@K for a node  $i$  and recommended node set  $\mathcal{V}_i$  is defined as

$$\text{VCMPR@K for node } i = \frac{\sum_{j \in \mathcal{V}_i} Y_{ij}}{\max(C, m_i)}, \quad (28)$$

where  $m_i$  is the number of true connections in the test data, i.e.,  $m_i = \sum_j Y_{ij}$ . We compute the average VCMPR@K for all nodes as the performance of the link prediction method for the graph. We observed that the degree-corrected benchmark provides method rankings more similar to those of the recommendation task measured by VCMPR@K than the standard and HearT benchmarks (Fig. 10).

#### E.6. Evaluation of the link prediction performance using Hits@K

Hits@K is another common metric used to evaluate link prediction methods alongside AUC-ROC. We investigated whether degree bias affects Hits@K scores and if our bias correction improves the correlation between Hits@K and actual link prediction performance. To compute Hits@K, we first ranked all test data edges by their predicted scores in descending order. We then counted the number of positive edges among the top K edges. This count was normalized by the maximum possible value (K) to indicate how close the method came to perfect prediction.

Our analysis revealed that the Hits@K scores for PA are consistently high across most networks, with only a few exceptions in networks with very low degree heterogeneity (Fig. 11A–D). The supiously high performance of PA remains consistent regardless of the K value used.

When we applied the same analysis to the degree-corrected benchmark, we found that the Hits@K scores for PA span the range between 0 to 1.0 (Fig. 11E–H). This indicates that the degree correction effectively mitigates spurious results and

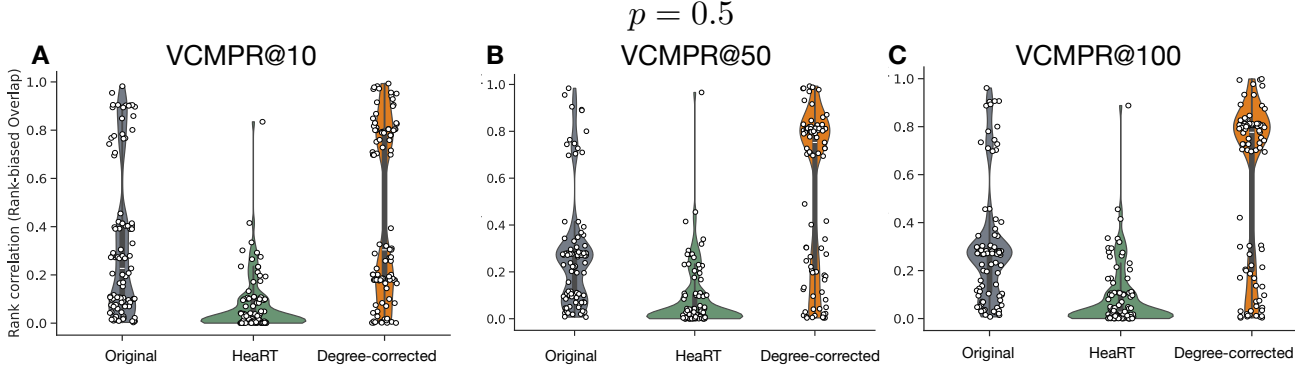


Figure 10. VCMPR@K for different K of recommendations.

prevents inflation of performance metrics due to degree bias.

We then compared the Hits@K scores with the actual link prediction performance, measured by NDCG@100, using RBO scores. Our results show that the RBO scores for the degree-corrected benchmark tend to be higher than those for the standard benchmark (Fig. 11I–L). This suggests that the degree-corrected benchmark provides a more accurate assessment of link prediction performance.

In summary, whether using AUC-ROC or ranking-based metrics like Hits@K, the underlying data used for evaluation is crucial. Our findings reveal a systemic problem: the data itself, when not properly corrected, has a bias that skews results in a way that is difficult to mitigate through metric selection alone. These results highlight the importance of addressing degree bias in link prediction evaluations, regardless of the metric used, and emphasize the need for careful evaluation methods in graph-based recommendation systems to ensure benchmark performance accurately reflects real-world performance.

#### E.7. Evaluation of the community detection performance using the normalized mutual information

Normalized Mutual Information (NMI) is a standard metric for assessing community detection methods (Lancichinetti & Fortunato, 2009; Fortunato & Hric, 2016). NMI quantifies the similarity between actual and predicted community assignments, where a score of zero indicates no similarity. We note that NMI has a bias favoring partitions with small communities (Gates et al., 2019), and thus, we used the element-centric similarity that does not have this bias in our main experiment. We note that NMI has a bias favoring partitions with small communities (Gates et al., 2019), and thus, we used the element-centric similarity that does not have this bias in our main experiment. Nevertheless, we include the results for NMI in Fig. 12 for comparison. As with the element-centric similarity, our results show that the degree-corrected GNNs perform on par or better than the original GNNs.

#### E.8. Sensitivity to the choice of the LFR benchmark parameters

We tested the robustness of the results by using different parameter values for the LFR benchmark. First, we confirmed the consistent results when varying the average degree  $\langle k \rangle$  from 25 to 50 (Fig. 13), or the maximum community size and degree from 1000 to 500 (Fig. 14).

### F. GNNs trained with the HeaRT benchmark

We compared our degree-corrected benchmark with the distance-aware HeaRT benchmark (Li et al., 2024a). We trained the GNNs using the negative samples generated by the HeaRT benchmark. Due to the computational expense of the negative sampling process of HeaRT, we selectively choose the LFR graphs with a small mixing rate ( $\mu = 0.1\text{--}0.20$ ), where communities are well-separated. If the benchmark facilitates the GNN’s learning of communities in networks, the performance of community detection must be at least as high as the original benchmark. Failure to do so indicates that the benchmark is not effective as a training method for learning community structure.

The results when training GNNs on the HeaRT benchmark showed notably lower performance compared to both the standard

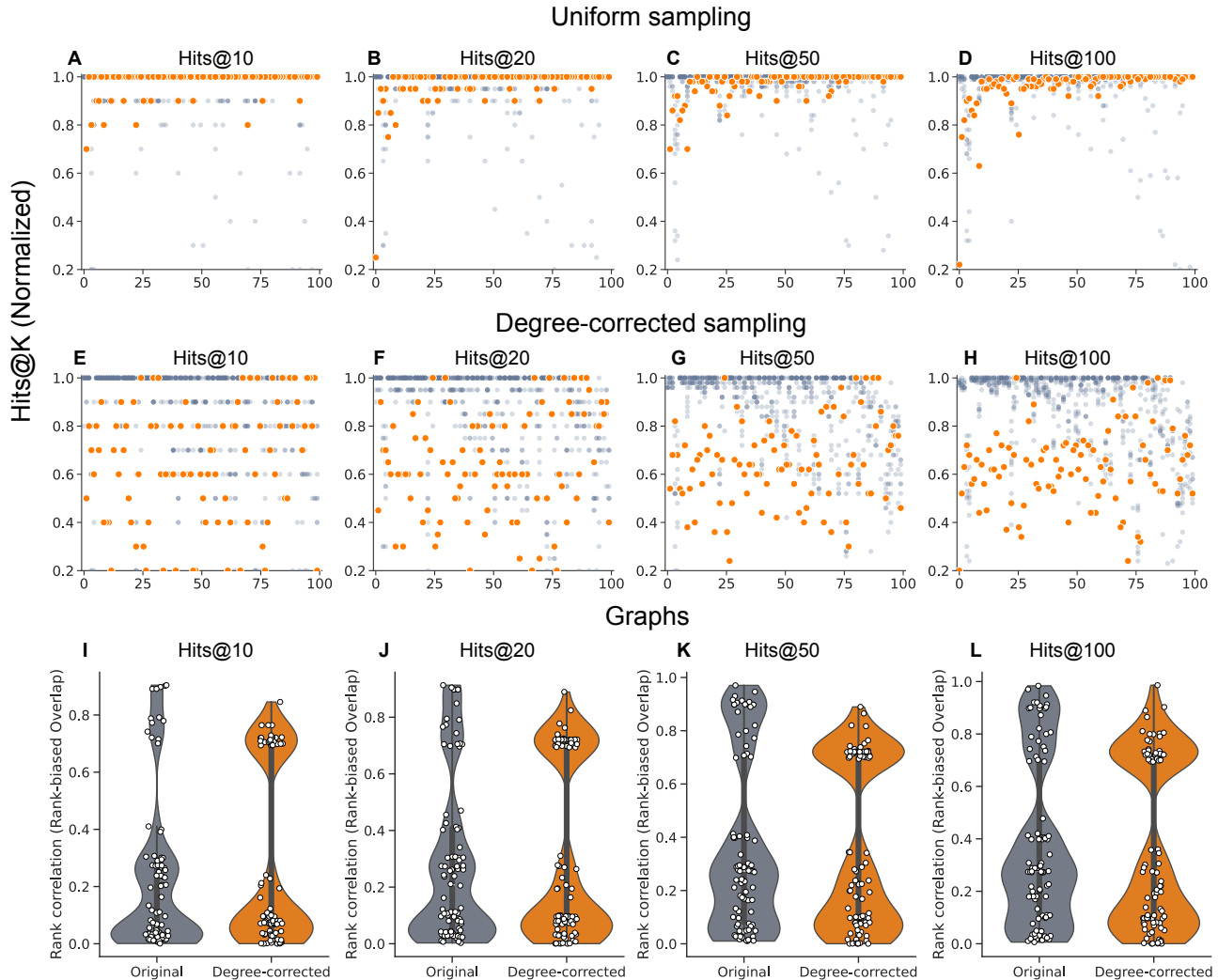


Figure 11. Link prediction performance using Hits@K. **A–D** Hits@K score for the PA model for the standard benchmark. **E–H** Hits@K score for the PA model for the degree-corrected benchmark. **I–L** The RBO score between the Hits@K scores and the recommendation performance measured by NDCG@100.

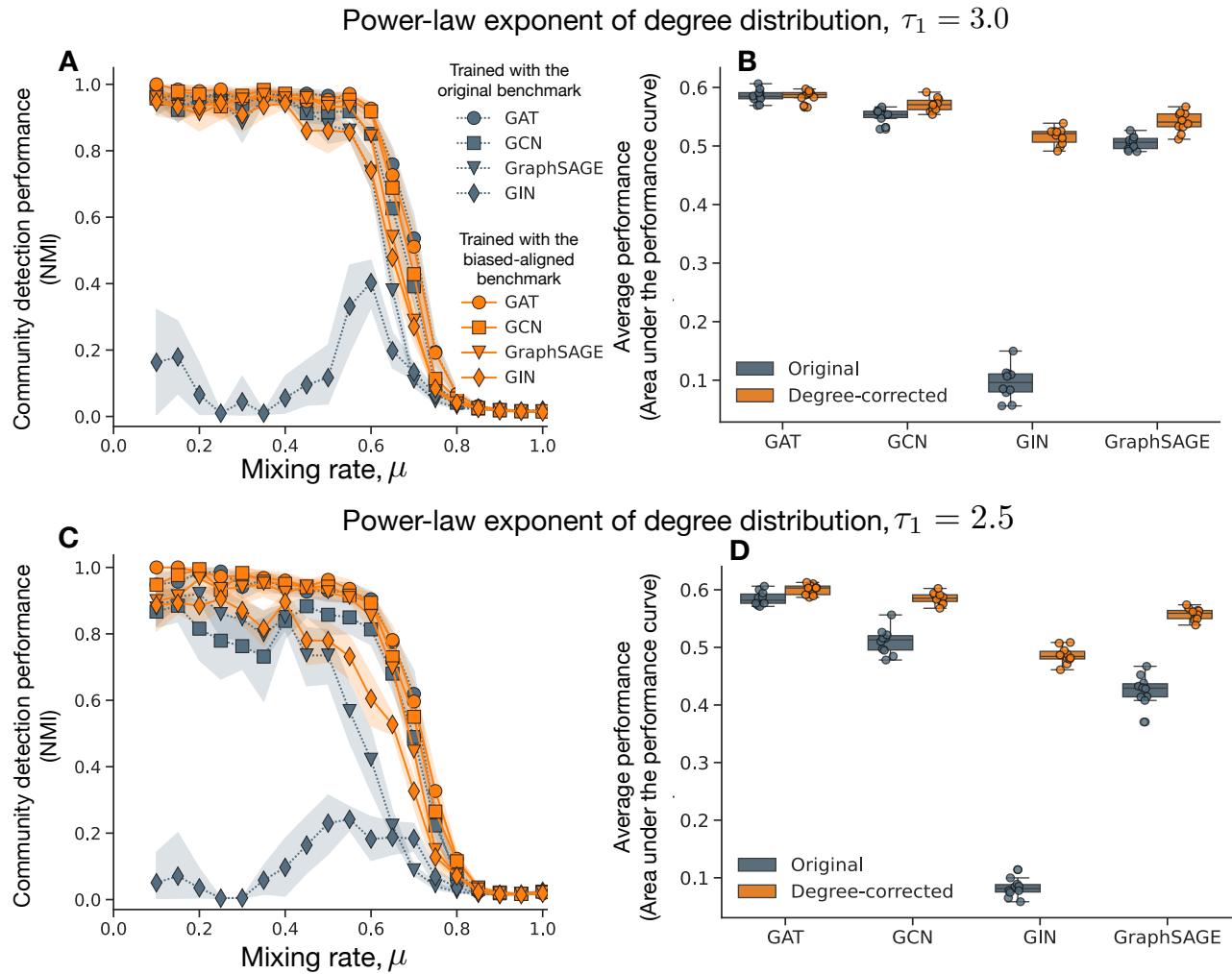


Figure 12. Performance of the GNNs on the LFR benchmark measured by NMI.

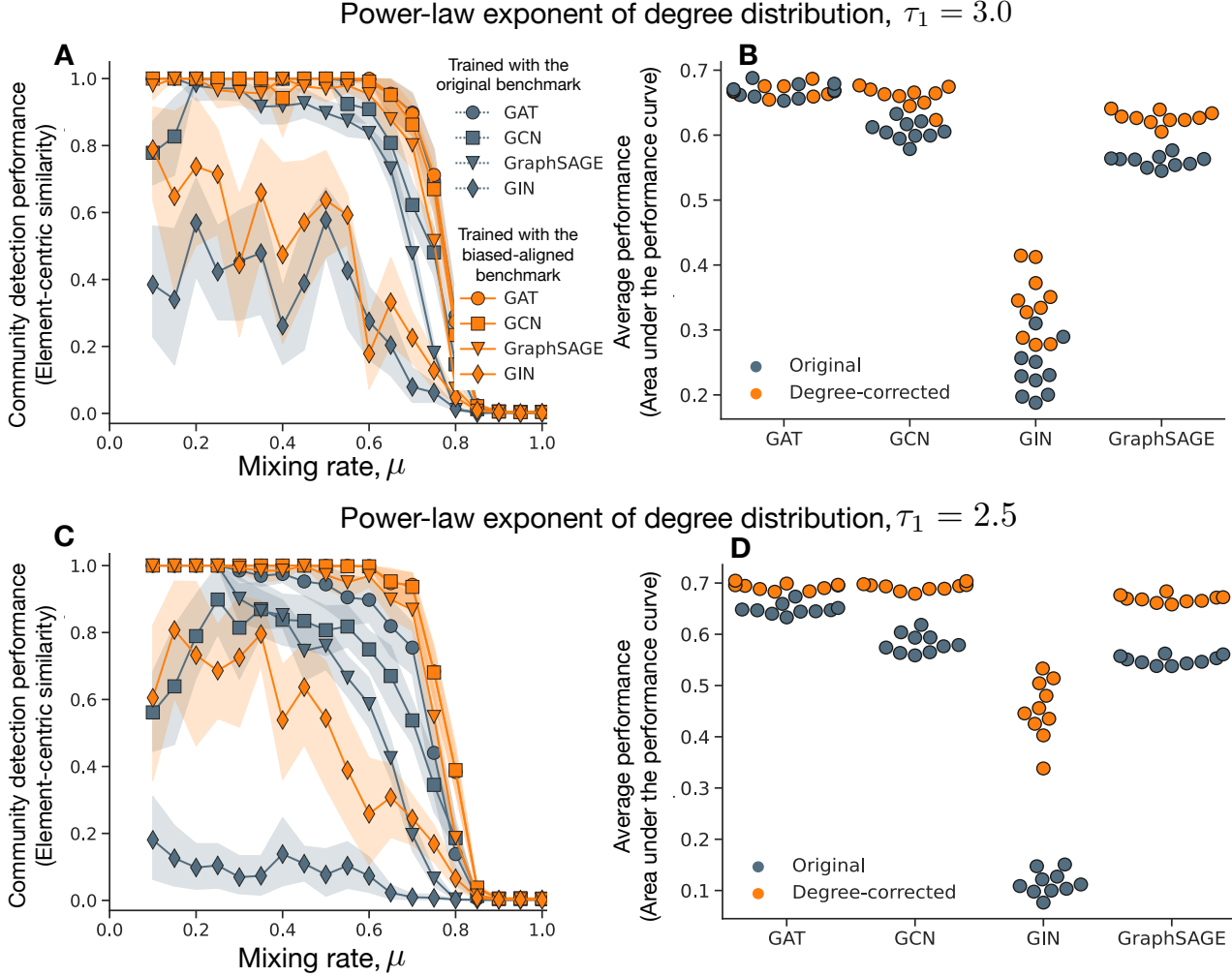


Figure 13. Performance of the GNNs on the LFR benchmark measured by NMI when varying the average degree  $\langle k \rangle$  from 25 to 50.

and degree-corrected benchmarks.

For comparison, the performance of GNNs trained on both the standard and degree-corrected benchmarks exceeded 0.2 within this range of mixing rates.

## G. Correlation between AUC-ROC and other network statistics

Figure 15A shows the correlation between AUC-ROC and other network statistics. We observed that the AUC-ROC of PA is strongly correlated with the degree heterogeneity in terms of the variance of the log-normal distribution of node degrees, more than other network statistics.

Figure 15B shows the correlation between AUC-ROC and the models that outperform PA on the standard benchmark. We observed that these models exhibit substantially weaker correlations between their AUC-ROC and degree heterogeneity, suggesting that their performance is not strongly tied to degree heterogeneity.

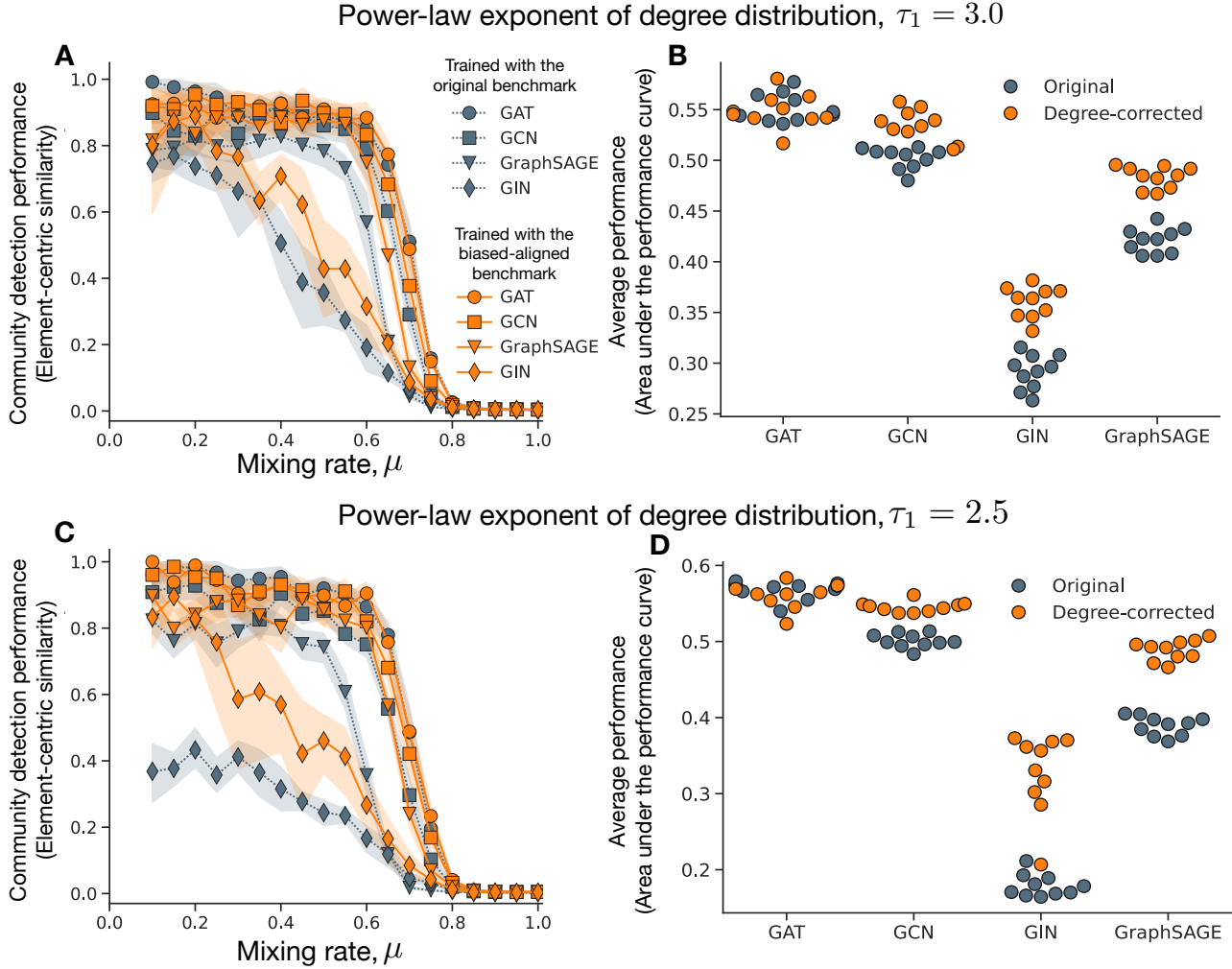


Figure 14. Performance of the GNNs on the LFR benchmark measured by NMI when varying the maximum community size and degree from 1000 to 500.

Table 3. Performance of GNNs trained using the HeaRT benchmark for networks with different mixing rates  $\mu$ .

Mixing rate	GAT	GCN	GIN	GraphSAGE
0.10	0.00668	0.04247	0.00603	-0.00063
0.15	0.01600	0.01383	0.02049	-0.00004
0.20	0.00951	0.01670	0.00955	-0.00023

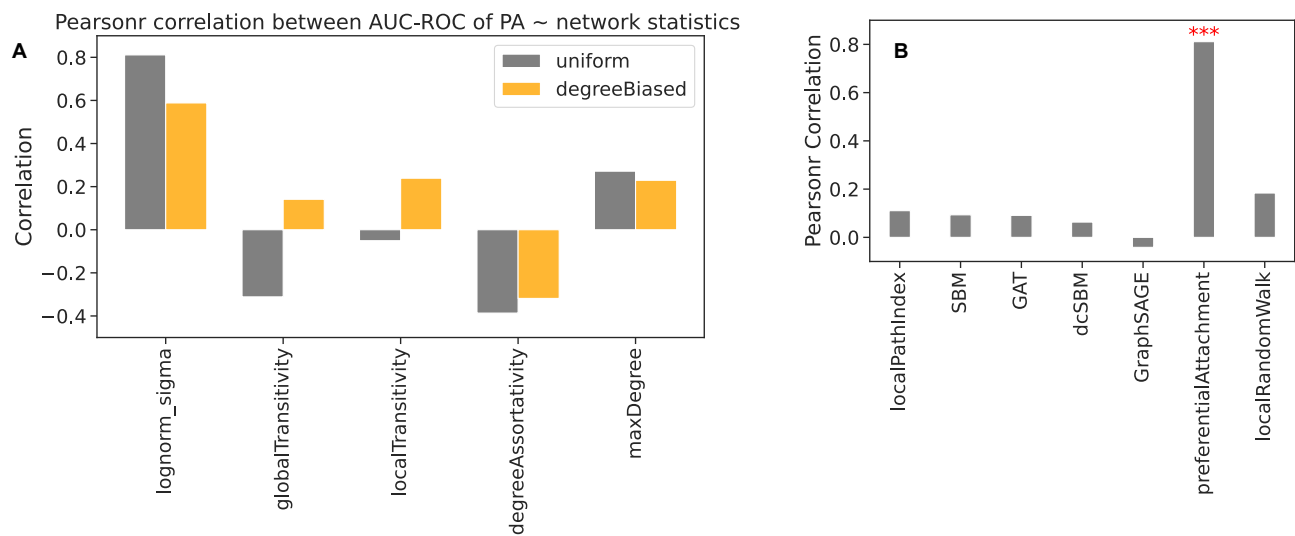


Figure 15. Correlation between AUC-ROC and other network statistics.

**Table 4.** Network data tested in this study. We consider social, technological, information, biological, and transportation (spatial) networks. For simplicity in our analysis, we consider these networks to be unweighted, undirected, and without self-loops. Variance refers to the variance of the node degrees. Assortativity refers to the degree assortativity, and Heterogeneity refers to the degree heterogeneity computed by (Jacob et al., 2017).

Network	Nodes	Edges	Max. Degree	Variance	Assortativity	Heterogeneity
Political books	105	441	25	29.69	-0.128	0.43
College football	115	613	12	0.78	0.162	0.20
High school 2011	126	1709	55	153.71	0.083	0.62
Food web bay wet	128	2075	110	249.17	-0.112	0.62
Food web bay dry	128	2106	110	249.85	-0.104	0.63
Radoslaw email	167	3250	139	993.84	-0.295	0.62
Highschool 2012	180	2220	56	120.37	0.046	0.51
Little Rock Lake	183	2434	105	433.29	-0.266	0.54
Jazz	198	2742	100	303.12	0.020	0.55
C. Elegans	297	2148	134	167.56	-0.163	0.38
Network science	379	914	34	15.42	-0.082	0.23
Dublin social	410	2765	50	70.51	0.226	0.29
Airport	500	2980	145	499.03	-0.268	0.35
Caltech	762	16651	248	1365.76	-0.066	0.42
Reed	962	18812	313	1254.53	0.023	0.38
Political blogs	1222	16714	351	1474.67	-0.221	0.34
Haverford	1446	59589	375	3687.70	0.067	0.41
Simmons	1510	32984	300	1288.53	-0.062	0.32
Swarthmore	1657	61049	577	3472.20	0.061	0.37
Petster	1788	12476	272	440.86	-0.089	0.24
UC Irvine	1893	13835	255	599.57	-0.188	0.24
Yeast	2224	6609	64	63.67	-0.105	0.15
Amherst	2235	90954	467	4007.71	0.058	0.35
Bowdoin	2250	84386	670	3206.35	0.056	0.33
Hamilton	2312	96393	602	3940.69	0.031	0.34
Adolescent health	2539	10455	27	18.59	0.251	0.10
Trinity	2613	111996	404	3742.49	0.072	0.32
USFCA	2672	65244	405	2041.31	0.092	0.27
Japanese book	2698	7995	725	608.58	-0.259	0.17
Williams	2788	112985	610	3901.94	0.040	0.32
Open flights	2905	15645	242	485.44	0.049	0.21
Oberlin	2920	89912	478	2838.11	0.050	0.28
Wellesley	2970	94899	746	3079.68	0.064	0.29
Smith	2970	97133	349	2432.51	0.044	0.28
Vassar	3068	119161	482	3453.23	0.101	0.30
Middlebury	3069	124607	473	3865.24	0.078	0.30

Table 5. (Continued) Network data tested in this study.

Network	Nodes	Edges	Max. Degree	Variance	Assortativity	Heterogeneity
Pepperdine	3440	152003	674	5695.91	0.055	0.31
Colgate	3482	155043	773	4009.14	0.067	0.29
Santa	3578	151747	1129	4933.35	0.071	0.29
Wesleyan	3591	138034	549	3548.92	0.095	0.28
Mich	3745	81901	419	1997.51	0.142	0.24
Bitcoin alpha	3775	14120	511	402.89	-0.169	0.17
Bucknell	3824	158863	506	3498.69	0.094	0.27
Brandeis	3887	137561	1972	4646.98	-0.026	0.27
Howard	4047	204850	1215	8506.41	0.058	0.32
Rice	4083	184826	581	5669.22	0.065	0.29
GR-QC 1993-2003	4158	13422	81	74.41	0.639	0.12
Tennis	4338	81865	451	4573.31	0.003	0.26
Rochester	4561	161403	1224	3632.47	0.025	0.25
Lehigh	5073	198346	973	4073.33	0.035	0.24
JohnsHopkins	5157	186572	886	4761.94	0.080	0.25
HT09	5352	18481	1287	1333.44	-0.431	0.14
Wake	5366	279186	1341	7469.92	0.071	0.27
Hep-Th 1995-99	5835	13815	50	20.77	0.185	0.08
Bitcoin OTC	5875	21489	795	531.22	-0.165	0.15
Reactome	5973	145778	855	4612.48	0.241	0.21
Jung	6120	50290	5655	16029.25	-0.233	0.16
Gnutella Aug 08 2002	6299	20776	97	72.95	0.036	0.11
American	6370	217654	930	3847.11	0.066	0.22
MIT	6402	251230	708	6241.81	0.120	0.24
JDK	6434	53658	5923	16112.86	-0.223	0.16
William	6472	266378	1124	5164.22	0.052	0.23
U Chicago	6561	208088	1624	4093.91	0.018	0.22
Princeton	6575	293307	628	6164.10	0.091	0.24
Carnegie	6621	249959	840	5674.47	0.122	0.24
Tufts	6672	249722	827	4525.50	0.118	0.22
UC	6810	155320	660	2297.32	0.125	0.19
Wikipedia elections	7066	100736	1065	3332.59	-0.083	0.21
English book	7377	44205	2568	3699.80	-0.237	0.16
Gnutella Aug 09 2002	8104	26008	102	66.74	0.033	0.09

Table 6. (Continued) Network data tested in this study.

Network	Nodes	Edges	Max. Degree	Variance	Assortativity	Heterogeneity
French book	8308	23832	1891	1217.86	-0.233	0.12
Hep-Th 1993-2003	8638	24806	65	41.61	0.239	0.08
Gnutella Aug 06 2002	8717	31525	115	51.87	0.052	0.09
Gnutella Aug 05 2002	8842	31837	88	54.66	0.015	0.09
PGP	10680	24316	205	65.24	0.238	0.09
Gnutella Aug 04 2002	10876	39994	103	48.65	-0.013	0.08
Hep-Ph 1993-2003	11204	117619	491	2307.04	0.630	0.16
Spanish book 1	11558	43050	2986	3353.23	-0.282	0.12
DBLP citations	12495	49563	709	284.34	-0.046	0.10
Spanish book 2	12643	55019	5169	6953.72	-0.290	0.11
Cond-Mat 1995-99	13861	44619	107	45.70	0.157	0.07
Astrophysics 1	14845	119652	360	472.92	0.228	0.11
Astrophysics 2	17903	196972	504	961.58	0.201	0.11
Cond-Mat 1993-2003	21363	91286	279	119.00	0.125	0.07
Gnutella Aug 25 2002	22663	54693	66	28.58	-0.173	0.04
Internet	22963	48436	2390	1085.20	-0.198	0.08
Thesaurus	23132	297094	1062	1993.31	-0.048	0.12
Cora	23166	89157	377	123.05	-0.055	0.07
AS Caida	26475	53381	2628	1113.83	-0.195	0.08
Gnutella Aug 24 2002	26498	65359	355	35.03	-0.008	0.04
ogbl-collab	232865	961883	382	178.857773	0.269877	1.134311
ogbl-ddi	4267	1067911	2234	176801.815426	0.037832	0.730724
ogbl-biokg-protein	11034	884042	2551	62766.451816	-0.027401	1.112268
ogbl-biokg-drug	7313	137027	652	15456.627212	0.079466	1.577354
ogbl-biokg-function	44635	1180424	17690	61471.922776	-0.128156	1.770447